MOLECULAR SELF-ASSEMBLY OF AROMATIC HYDROCARBON DERIVATIVES AT SOLID-LIQUID INTERFACES

A THESIS SUBMITTED TO THE GRADUATE SCHOOL IN PARTIAL FULFILLMENT OF THE REQUIREMENTS FOR THE DEGREE OF MASTER OF SCIENCE

CODY WESLEY LEASOR

DR. ZHIHAI LI-ADVISOR

BALL STATE UNIVERSITY

MUNCIE, INDIANA

JULY 2019

ACKNOWLEDGEMENTS

Thank you, to all my friends and family. Without the constant love and support I would not be where I am today, and I would certainly not be who I am today. I am quite lucky to have been a graduate student in Ball State University's Chemistry Department. The range of faculty/staff and fellow students are filled with amazing and kind people, many of which have become great friends of mine.

To my fellow graduate students, it was an amazing two years and I wish we had more time together. You have all been so nice in welcoming me into the Chemistry Department and into your lives. Thank you for helping me out whenever I became ill and always being there to help with discussions or consultations. I will miss our weekly shenanigans with game nights to decompress from our graduate studies.

To the faculty/staff of Ball State University's Chemistry Department, I have had the pleasure of interacting with most, if not all, members of the Chemistry Department. I want to say thank you, each faculty/staff member that I have interacted with has either taught me something valuable with my career in chemistry, helped me get to the next step in my career, or both. I would like to also thank Dr. Zhihai Li, who has been very patient, caring, and an amazing advisor, instructor, and friend to me the past two years. You have helped me become the scientist I am today, thank you.

To my family, thank you for supporting me in the path I have chosen and the goals I am pursuing. I hope to make you all proud in my current and future endeavors. I will never forget all that you have done or continue to do for me. I love you all and thank you so very much!

ABSTRACT

Electrochemical (EC) Scanning Tunneling Microscopy and Cyclic Voltammetry was used to study the adsorption/self-assembly of Benzoic Acid (BZA) in either 0.05 M H_2SO_4 or 0.1 M $HClO_4$ electrolyte solutions on a Au(111) substrate. BZA, unlike similar compounds, presents a challenge to form long-range ordered nanostructures, because it only has one functional group that allows for hydrogen-bonding. Therefore, the intermolecular interactions are relatively weak and molecule-substrate interaction become more critical. Observations of long-range nanostructures of BZA at these electrode/electrolyte interfaces was difficult in 0.05 M H_2SO_4 from competing adsorption of sulfate ions. 0.1 M $HClO_4$ electrolyte was then used where changing the concentration of BZA had a large role in the formation of adsorption phases. Where, at/greater than 6 mM BZA revealed four different regions of adsorption phases, while at less concentrations revealed disordered phases. EC potential also played a crucial role in this study, and different nanostructure are revealed depending on the EC potentials applied.

DEDICATION

For my mother; who has raised me and to whom I owe my life. You are the one that taught me to never settle for anything except for my best and to constantly want more out of myself which led me to where I am today. Thank you, and I love you mom.

TABLE OF CONTENTS

CHAPTER 1: BACKGROUND AND INTRODUCTION

1.1: SURFACE PHENOMENA FROM NATURE

There is a tremendous amount of information that we can learn from nature. One area of nature that we can study is that of surfaces. Numerous reactions take place between surfaces or between two types of phases of matter, depending on preferential perspective. Take a Lotus leaf for example, it is claimed to be self-cleaning, however, what makes it self-cleaning is the surface of the leaf that forms a hydrophobic layer. This outer layer will prevent water from absorbing onto the leaf and cause water to trickle off, collecting dirt as it passes.[1-2]

Another fascinating tribute to nature is the common gecko; a gecko has the ability to scale walls and even run across a ceiling while being completely upside down. This is due to the gecko's palm having a microscale structure that allows for gripping small surfaces that gives it the ability to climb objects well.[2-3] In both examples that have been listed, the common factor is the relationship between surfaces that allows for different actions to be achieved.

1.2: SUPRAMOLECULAR CHEMISTRY AND SURFACE ASSEMBLY

These tributes to nature can be studied through the field of nanoscience, or more accurately, through the study of two-dimensional nanostructures found as the interaction of the surfaces. This project, however, will be studying the surface interaction between a solid and liquid interface, and therefore, more like the example of the Lotus leaf. Unlike the lotus leaf, this project will not be studying hydrophobicity or avenues of self-cleaning surfaces. Instead, this project focuses on how certain molecules in the liquid phase interact with an atomically flat solid surface. In this interaction there is a type of binding between the solid surface and the molecules found within the solution that is in direct contact with the solid, this interaction is known as adsorption.

Adsorption is the chemical or physical binding of molecules onto a surface.[4-5] Typically, this attraction is due to intermolecular forces, such as dipole-dipole forces, hydrogen bonding, London dispersion forces, and etc.[4-5] The goal of this project is to observe the adlayer that forms at the solid surface. The study probes the type of adlayer that can form long range patterns of multiple molecules that are either a specific orientation or a mixture of different orientations. In essence, we strive to determine the mechanism by which these molecules arrange themselves into long range patterns, that is, the formation and self-assembly of the supramolecular two-dimensional nanostructures.

Supramolecular chemistry is a term that can be found within multiple topics of chemistry that is used to describe a type of complex made of either one large enough molecule that allows for intermolecular interactions or multiple molecules that allow for similar interactions that promote an architecture of intermolecular forces.[4] The supramolecular complexes or nanostructures (referring to the two observations as images produced in this project or previous works) are held together mostly by noncovalent interactions, possibly, through the following intermolecular forces: hydrogen bonds between polar groups[6-8], X-bonding (where X is a halogen)[9], and Van Der Waals interaction such as London Dispersion forces[10-11]. These bindings take less energy to break than a covalent bond. Yet, even though they are not as strong as covalent bonds, the large number of these weak interactions that are present stabilize the assembly of the molecules to form a Supramolecular Nanostructure (SN). Nonetheless, the title of this thesis has the term “self-assembly” which is referring to the formation of SNs. This term is not referring to the molecules spontaneously adsorbing onto the surface but refers to applying a potential that induces the adsorption of molecules to form long-range patterns onto the solid surface, which in this case, is an atomically flat metal substrate.

1.3: MOLECULES OF INTEREST AND THEIR FUNDAMENTAL INFORMATION

Nature has complex works of art like the lotus and the gecko's palm. In these complex examples, there are still a large number of compounds that make up the surfaces that allow the lotus leaf to be self-cleaning and the gecko's palm to scale walls. To be more detailed is to try and focus in and to look at a surface to make observations of the surface's molecular building blocks. That is what this project aims to do is to study parameters that effects the formation of the SNs. Additionally, determining the molecule-molecule and molecule-substrate interactions that dictate the formation of the SNs. Unfortunately, starting with something as complex as the previous two examples is not ideal. Instead the molecules of interest are derivatives of benzene, naphthalene, and pyrene.

This project is a fundamental collection of information on the interaction of the derivatives of these compounds with the substrate. Yet the novelty or unique feature of this project that sets it apart from other works is that this study is at the solid-liquid interface using a single building block, which for this project is benzoic acid (BZA), on Au(111) to explore the effects/parameters that influence the formation of the SNs. As a result, the derivatives of naphthalene and pyrene will also have Carboxylic Acid Functional Groups (CAFGs), like BZA. Thus, the molecules of interest are BZA, 2,6-naphthalenedicarboxylic acid (2,6-NA), 2,7-naphthalenedicarboxylic acid (2,7-NA), and 1,6-pyrenedicarboxylic acid (1,6-PyA).

BZA	2,6-NA	2,7-NA
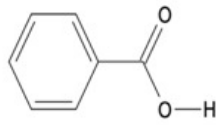	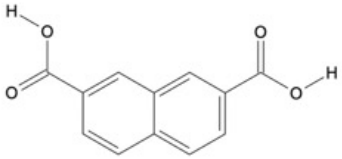	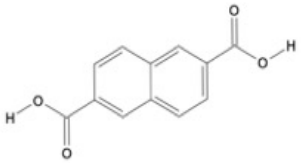

Figure 1.1: ChemDraw molecular structures of BZA (A), 2,6-NA (B), 2,7-NA (C), and 1,6-PyA (D) which are referred to as the molecules of interest.

1.4: SPECIFYING THE PROJECT AND LITERATURE REVIEW

BZA seen in Figure 1.1, and its interaction with the metal substrate, which is a Gold (Au) substrate, more specifically Au(111), have been studied by the use of Scanning Tunneling Microscopy (STM); where in this work BZA has been the focus for the past two years of this project and perhaps other molecules might be studied past the point of this graduate student. Throughout the experiments that have been done in the past two years, there has been a list of goals for each molecule of interest. These goals were to observe the long range ordered (pattern) SNs of BZA on a Au substrate, the effects of the formation of the SNs, and the functional group position on the base unit of the molecule of interest. If there is a disordered (no discernable pattern) with the adsorbed species, then none of the other goals can be achieved because position/orientation of the adsorbed species cannot be observed. The formation of SNs, however, can be influenced by the effects of three parameters, where the goal here is to understand the following parameter effects: electrolyte solution effect, the effect of the potential that is applied to the sample, and the effect of the concentration of BZA ([BZA]). Where the experiments explore these goals and effects done on top of the substrate that is atomically flat with a face-centered cell (fcc) that has a surface known as 1,1,1 (111), see Figure 1.2.

Additionally, in the exploration of the SNs of BZA, it was thought to lead to the understanding of the molecule-substrate and the molecule-molecule interactions within the formation of the SNs. Where the molecule-molecule interactions might be highly dictated on the possible amount of hydrogen bonding that can occur with the CAFG. Theoretically, the more CAFGs on the benzene ring the more hydrogen bonding that can occur and thus make it easier to observe long range SNs. This leads to the anticipation that perhaps BZA is difficult to observe the SNs in comparison to benzene derivatives with multiple CAFGs.[6-7]

Once BZA hydrogen bonds to another BZA molecule, there is no other location for hydrogen bonding to occur. Thus, a chain or network of hydrogen bonded molecules cannot be formed.

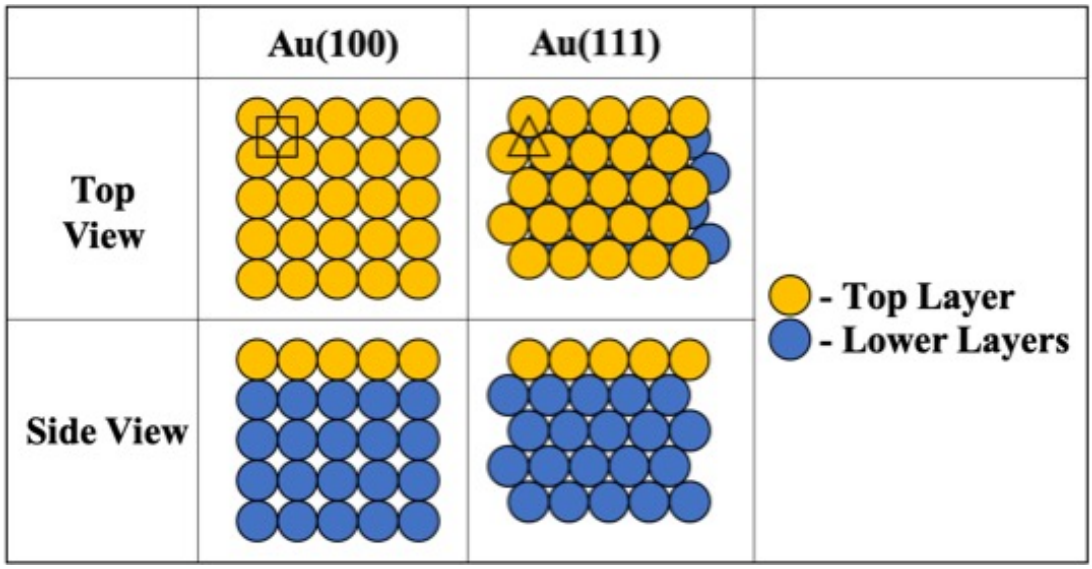

Figure 1.2: PowerPoint drawings of the top and side view of the Au crystal lattices 1,0,0 (100) and 1,1,1 (111).

Finally, once all of the goals have been met for one molecule of interest, the next step would be to repeat all of the goals previously listed, with a mixture of at least two different molecules. Where at one molecule is a molecule of interest and the other molecule would be a compound that similar

to BZA that has already been studied well under similar conditions. For example, 1,3,5-benzenetricarboxylic acid (Trimesic Acid, TMA) and BZA at a mole ratio of 1 TMA to 3 BZA, 1:2, and 1:1.

Compounds like Trimesic Acid (TMA) and Isophthalic Acid (IA) have already been extensively studied individually with the use of STM[6-7]. In fact, there are a great number of published works with various compounds studied with STM. Before we delve into those works, it must be known that STM can be worked under three common systems. These systems are under ambient conditions (otherwise known as "in-air"), under Ultra-High Vacuum (UHV) conditions, and under electrochemical (EC) conditions, see Figure 1.3.

When EC conditions, is coupled with STM the technique is often abbreviated as EC-STM. These systems can have a pivotal impact on an experiment ran under a specified condition. For example, if there is an experiment that calls for a study to be done at extremely low concentrations of a compound onto a substrate, in a very clean environment, and at a certain (lower) pressure then the UHV condition will probably be chosen over in-air STM or EC-STM. For example, the study of Naphthalene on Cu(111) under UHV STM[12].

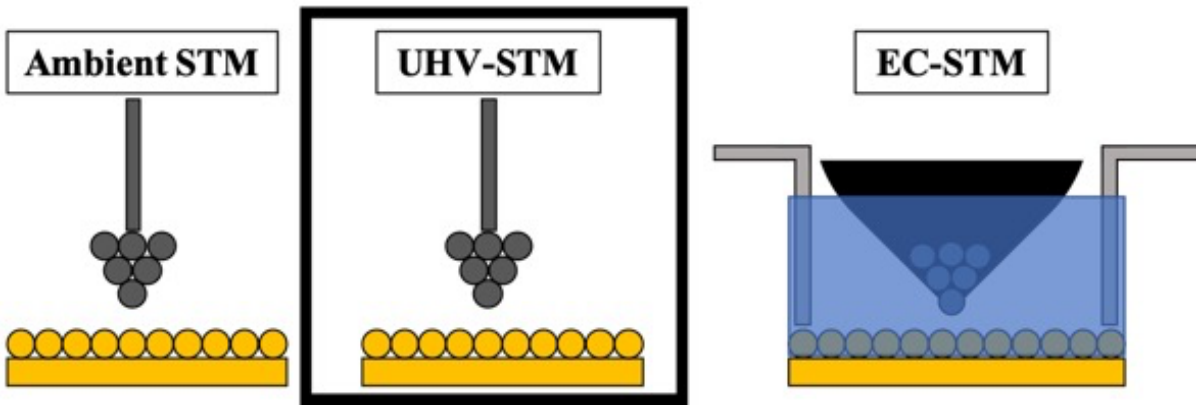

Figure 1.3: The three STM Environments drawn with PowerPoint drawing of the three STM environments.

There is yet another factor that could have an impact on experiments that are not dependent on the systems/conditions listed above. This factor is the substrate; the substrate can be any metal or any solid that is both conductive and can be manipulated so that it is atomically flat. Such substrates are often seen as one of the noble metals or seen as a solid compound with a crystal lattice that is relatively flat. Examples of substrates are copper (Cu), silver (Ag), Au, Titanium (IV) Oxide or Titanium Dioxide (TiO_2), Highly Orientated Pyrolytic Graphite (HOPG), etc.[6, 11, 13-15] The substrate that will be used the most throughout the following project is Au. This is due to the inert nature of Au (so that an unwanted reaction will not occur), and the convenience of making it atomically flat, which will be covered in Chapter 4.

The Au substrate can be used throughout all systems/conditions of STM, however, this project will utilize Au for the EC-STM system.[6, 16-17] There have been plenty of published works that use a Au substrate under ambient or UHV conditions.[16-17] These studies have much to offer with regards to studying molecule-molecule interactions, molecule-substrate interactions, and/or studying the substrate without any adsorbed species on its surface or very few molecules adsorbed to its surface. For example, one study was done under ambient conditions with a Au substrate to examine the growth of islands with the use of thiolated Au Nanoparticles (NP)[16]. Another example, is of a study under UHV conditions with a Au(111) substrate that examined how nonacene generates on the Au surface from tetrahydronanacene[18]. The second example is a great demonstration of how Au nanoparticles can be used for synthesis-based reaction. This also shows how different information can be retrieved with either STM or Atomic Force Microscopy (AFM).

AFM does not require the substrate or the sample on the substrate to be conductive; this is one of the major differences between AFM and STM. This project will primarily focus on the STM type of probing techniques, where the EC-STM requires the substrate and the solution that sits on

top of the substrate to be conductive. EC-STM offers more information to be taken from a sample than just the images that can be produced. Due to the fact that this system is under EC conditions, it gives the opportunity to study the EC potential of a substrate and of compounds that could interact with the substrate. This type of study is done throughout this project with the use of CV. In most cases, CV is a technique used to study the oxidation and reduction potentials of a given compound.

One such example is that found in Figure 1.4, where 1:1 volume ratio of 0.1M [$K_3Fe(CN)_6$] and 0.1M [$K_4Fe(CN)_6$] solution was used to measure three CVs. Where these CVs have different scan speeds, which are 50 mV/s (black line), 100 mV/s (red line), and 500 mV/s. The counter and reference electrodes were platinum wires and the working electrode was Ag|AgCl electrode. Note, that there had already been CV studies with respect to these compounds.[19-20] However, this data was collected through Advanced Analytical (Chem. 626) lab.

Unfortunately, the data was not saved correctly which led to a result for receiving data from the instructor so that the data was analyzed by the students who had similar issues. Therefore, Figure 1.4 was processed and analyzed by Cody Leasor after it was received from the instructor.

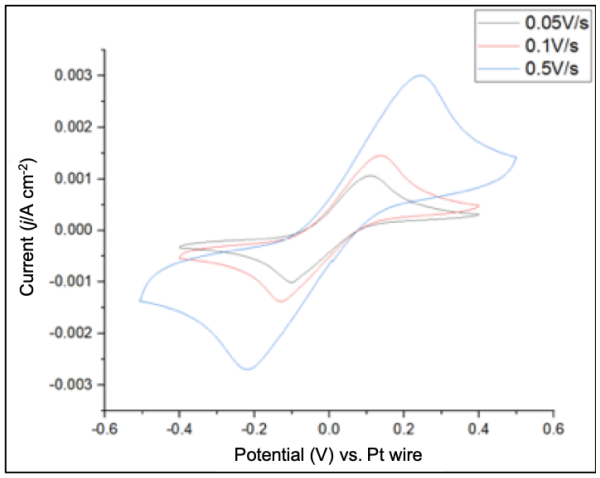

Figure 1.4: EC quasi-reversible CV of 1:1 volume ratio of 0.1 M [$K_3Fe(CN)_6$] and 0.1 M [$K_4Fe(CN)_6$].

Alternatively, CV is also used to study different types of SNs that form based on the potential applied to the substrate (also known as the sample potential), the unit cell of the substrate, and the compounds that are interacting with the substrate. This will be covered in Chapter 2.

Take the two studies of Benzene, Naphthalene, and Anthracene on Cu(111) surface and Pyrene and Perylene on Cu(111) for example.[10-11] In these works, the authors provide CVs that were ran under EC-STM that contain no peaks between the oxidation and reduction potentials.[10-11, 21] This suggests that the molecules only have one way of arranging themselves onto the substrate within the potential windows, additionally, based on the images that were observed, it suggests that van der Waals forces play the main role in the molecule-molecule interactions due to the functional groups (or lack of functional groups) on the aromatic rings. If there were more than one way to arrange the molecules on the surface, then one might postulate that there would be more peaks in the CV. A non-oxidation/reduction peak (an adsorption/desorption peak) corresponds to the phase transition between two SNs. So, if there were two ways for a compound to arrange itself on the substrate, then theoretically, there would be one adsorption/desorption peak in the anodic and cathodic scans. These adsorption/desorption peaks are most likely found in between the two potentials that the substrate will either be oxidized or reduced.

It is postulated that some of the largest contributors to the formation of different SNs are the functional groups on a given unit compound. Take BZA for example, the aromatic phenyl ring is the unit compound and the functional group is the one carboxylic acid group attached to the ring. It can be seen in the previous studies that the compounds are all aromatic ring structures without any other functional groups.[10-11] This leads to a minimal amount of SNs available to study. As a result, the more compounds with functional groups that allow for intermolecular interactions, such as hydrogen bonding, then it is more likely that those compounds have more SNs that will be

available to observe. This is the purpose behind choosing compounds that have CAFGs for the molecules of interest throughout this project.

There are other works, however, that use the same STM system/condition and even the same substrate used in this study, but with a different molecules and purpose. One such study was focused on fuel cell electrocatalysts to provide a novel O_2 reduction and the oxidation of H_2 and methanol.[22] This was done by using a Au substrate with Platinum (Pt) atoms deposited on top of the Au(111) surface in comparison with Pd(111) and Ru(0001).[22] This study utilized techniques with EC-STM, CV, Transmission Electron Microscopy (TEM), and other techniques that are not relevant to this project. Even though this published work is a great idea that is directed towards a cleaner energy source, it serves as a great way to show how other methods and techniques can be implemented throughout this type of research to give a new perception within a given field of study.

The purpose of this literature review is to provide the resources to make predictions. For example, any study with EC-STM that focuses on aromatic hydrocarbons without any other functional groups that adsorbed onto the surface of a noble metal, allows one to predict that there is not going to be any adsorption/desorption peaks because there is only one way for the compounds to arrange themselves on the surface of the substrate. Fortunately, this project has a higher complexity to it than a study that focuses on the base molecules of benzene, naphthalene, and pyrene.

To make predictions based on the molecules of interest, there must be a review of more literature that revolves around the topic of different carboxylic acids that form SNs under EC-STM conditions on a Au(111) surface. Fortunately, there are multiple published works in this area that will allow for such predictions. From a logical standpoint, let's start from the smallest set of

molecules and work up to larger sets of molecules. The smallest set of molecules should be derivatives of benzene rather than derivatives of naphthalene or larger aromatic hydrocarbons.

Arguably, the best starting point would be an EC-STM study of BZA on a Au(111) surface, however, this type of study has already been published. Where T.H. Vu and T. Wandlowski's 2017 work studies 12 mM BZA in 0.1 M $HClO_4$ under EC-STM, however, in this work there is no mention of an electrolyte effect even though $HClO_4$ electrolyte was used instead of H_2SO_4 electrolyte.[23] Additionally, it was mentioned that perhaps the lack of order structures observed for lower concentrations of BZA is due to the concentration.[23] Yet, this effect was not explored in this work, instead they made all of their observations of EC-STM images at 12 mM BZA in 0.1 M $HClO_4$.[23] However, in their 2016 work with BZA is explored in a similar system, where the difference between the two works is that the substrate is Au(100) instead of Au(111).[24] Whereas, Y. G. Kim et. al. also worked with BZA, terephthalic acid, and pyrazine on Pt(111) with EC-STM.[25] However in this work the concentration of BZA that was used was relatively low, at 0.1 mM, in comparison to this project and other works with BZA.[25]

Fortunately, this project will focus more on the three effects on the formation and observations of long range SNs with BZA. The next logical choice of a molecule of interest would be a benzene ring with two CAFGs, rather than just one. There are three options at this point, benzene-1,4-dicarboxylic acid also known as Terephthalic Acid (TA), benzene-1,3-dicarboxylic acid also known as Isophthalic Acid (IA), and benzene-1,2-dicarboxylic acid also known as Phthalic Acid (PA). S. Clair et. al. observed TA SNs; however, it was under UHV-STM. Perhaps, due to the lack of solubility of TA in water is a reason as to why there are not as many works with it in EC conditions.[26] However, Isophthalic acid has been studied under EC conditions and there are two main SNs that were produced.[7] The first, was at an applied potential to the substrate (or

sample) of 0.10 Volts (V) with the quasi-reference electrode of a Pt wire, where there is a zig-zag long range pattern that is observed when the SN.[7] It was proposed that this pattern was observed due to the formation of a dimer chain held together by hydrogen bonding at each of the two CAFGs positions interacting with the next and previous molecules' functional groups.[7]

Alternatively, the other SN that was observed took EC and thermal annealing to allow for the long-range linear type of patterns to develop.[7] This linear pattern was seen to have a higher surface coverage than the first SN; this was because the first SN had an orientation that was flat on top of the substrate, whereas, the second SN had an upright or slightly tilted orientation on the substrate.[7] The upright/tilted orientation was due to a covalent bond that forms between the two oxygen atoms in one of the CAFGs after deprotonation of the same functional group that interacts with the substrate.[7] These two SNs can be seen as the molecule-molecule and molecule-substrate interactions that were induced by the applied potential and formed due to hydrogen bonding and annealing effects. Yet, there are not as many works with PA which is possibly due to the instability of the SNs due to the position of the CAFGs.

The next logical molecule is TMA, where the three CAFGs that are attached to a benzene ring are evenly spaced apart. Unlike the work done with IA, this work with TMA shows five SNs.[6] Where the first four SNs have a flat orientation and the fifth SN has an upright/tilted orientation with respect to the substrate.[6] Similarly, to IA, these orientations are dependent on the potential applied to the sample whether they are more positive or negative potentials.[6-7] Interestingly, there is not as many peaks observed in the CV of TMA in 0.05 M H_2SO_4 electrolyte solution as one might expect. In fact, the first three SNs are found at potentials that come before the first phase change peak in the CV.[6] These SNs and the SN just after the first peak (fourth SN) are all formed

from molecule-molecule hydrogen bonding interactions that give the following long-range patterns: honeycomb, ribbon-type, herringbone, and linear dimers.[6]

The honeycomb pattern forms due to each of the three CAFGs interacting with three other TMA molecules, which is perpetuated throughout the covered surface.[6] This type of pattern is seen quite frequently throughout other studies and is not limited to the functional group; however, it is likely due to the number of locations where intermolecular reactions can occur and if they are evenly spaced apart.[6, 27] The ribbon-type pattern is formed from two of the three CAFGs interacting with two other TMA molecules.[6] This type of interaction allows for the formation of the proposed tetramer.[6] The herringbone pattern is formed from one of the three CAFGs interacting with only one TMA molecule, that results in a dimer.[6] The fourth SN that has the linear dimer pattern, where this pattern is much like it sounds, straight chains of dimers .[6] Much like the herringbone pattern, there is a dimer formation in the linear dimer pattern, however, the way the dimers arrange themselves are in a straight line rather than being ninety degrees from dimer to dimer.[6]

From the work with IA and TMA the SNs found allows for a prediction that can be made. For example, in the work with IA, it was observed that with a more positive potential applied to the sample there was a pattern of a flat orientation, much like the first four patterns observed in the work with TMA, and with a more negative potential applied to the sample there should be an upright orientation of TMA interacting with the substrate much like IA did at a similar potential allowing for a higher surface coverage pattern than any of the other patterns observed with TMA. This long-winded prediction would be correct. It can be seen that an upright/tilted orientation of TMA molecules is formed at a more negative potential, with a higher surface coverage than any other TMA pattern before it.

1.5: PROJECT MOTIVATION AND PURPOSE

Now that the general background information about this project has been covered, it would be an optimal time to discuss, and more directly specify, the motivation and purpose behind this project. The motivation of the research is to add to the fundamental information of aromatic hydrocarbons binding to the Au(111) substrate. Such that the molecule-molecule and molecule-substrate interactions can be compared to known characteristics of a compound. For example, the crystal structure of benzoic acid. The investigation of the compounds of interest were done by studying how potential dependency might affect the formation and manipulation of two-dimensional nanostructures on Au(111).

The purpose of this project, however, is not to apply the knowledge that is gained from each experiment to a real-world application, due to its fundamental nature. This fundamental project is to first explore how the adsorption phases of BZA can be influenced by the applied potential so that this information might add to surface corrosion[28] through the way benzoic acid adlayers form on a metal substrate, asymmetric heterogeneous catalysis[29] based on the BZA orientation and distribution on the metal surface, electrochemical sensors[30] and degradation of organic pollutants[31] through adsorption phases and Self-Assembled Monolayers (SAMs), surface-catalyzed reactions[32-33], and charge transfer in molecular devices[34]. In order to hypothesize or study by experimentation of the topics listed above, one first has to know how BZA will adsorb onto a specific metal substrate. Such that, the adlayers that are formed can be understood and manipulated for their respective studies.

1.6: PROJECT APPROACH AND PHILOSOPHY

The approach to this project will be done by using EC-STM on a Au(111) substrate where various concentrations of an aromatic hydrocarbon will be dissolved in a dilute electrolyte

solution. EC-STM allows for in situ observations by producing images of the solid-liquid phase boundary of the adlayers on the Au surface. This project starts by focusing on the smallest AH compound within the molecules of interest, BZA. This comes with some challenges, which was mentioned in section 1.4.

These challenges can be overcome by producing excellent probes/tips (atomically sharp and well-insulated by polymers), high-purity solutions and the STM cell, and using optimized parameters and stable equipment which include smaller tip-drifting or thermal movement of STM tip and substrate. As a result, the approach includes probe development and the improvement to the cleanliness of the general procedure. Additionally, the type of functional groups can have a direct influence on the formation of SNs, due to the fact they form from intermolecular interactions. Using functional groups that allow for hydrogen bonding (the strongest intermolecular interaction) have been understood to produce more SNs compared to an aromatic ring without any other functional groups.

This project also included the development of a method for the instrument, which incorporated the optimization of a probe fabrication technique, the development of a procedure for the synthesis of STM probes that yields consistently high-quality probes. Next, was the development of a procedure that would minimize the possibility of contamination. Optimization of the experimental conditions involved CV of various concentrations of BZA in either 0.05 M H_2SO_4 or 0.1 M $HClO_4$ electrolyte solutions and STM imaging of these solutions. Where first, there is a collection of CVs that help relate the electrolyte, BZA concentration, and EC potential applied to the substrate to the adsorption regions of BZA in either 0.05 M H_2SO_4 or 0.1 M $HClO_4$ on Au(111).

1.7: CHAPTER ONE REFERENCES

1. Barthlott, W.; Neinhuis, C., Purity of the sacred lotus, or escape from contamination in biological surfaces. *Planta* **1997,** *202*, 1-8.
2. Forbes, P., Self-cleaning Materials. *SciAm.* **2008,** *299* (2), 88-95.
3. Geim, A. K.; Dubonos, S. V.; Grigorieva, I. V.; Novoselov, K. S.; Zhukov, A. A.; Shapoval, S. Y., Microfabricated adhesive mimicking gecko foot-hair. *Nat. Mater.* **2003,** *2* (7).
4. Atkins, P.; De Paula, J., *Physical Chemistry*. Ninth ed.; Oxford University Press: Great Britain, 2010.
5. Zumdahl, S. S.; Zumdalh, S. A., *Chemistry*. Eighth ed.; 2010.
6. Li, Z.; Wan, L. J.; Wandlowski, T., Supramolecular Nanostructures of 1,3,5-Benzene-tricarboxylic Acid at Electrified Au(111)/0.05M H_2SO_4 Interfaces: An in Situ Scanning Tunneling Microscopy Study. *Langmuir* **2005,** *21* (15), 6915-6928.
7. Li, Z.; Wandlowski, T., Structure Formation and Annealing of Isophthalic Acid at the Electrcochemical Au(111)-Electrolyte Interface. *J Phys Chem C* **2009,** *113*, 5.
8. Addou, R.; Batzill, M., Defects and Domain Boundaries in Self-Assembled Terephthalic Acid (TPA) Monolayers on CVD-Grown Graphene on Pt(111). *Langmuir* **2013,** *29* (21), 6354-6360.
9. Pham, T. A.; Song, F.; Nguyen, M. T.; Stohr, M., Self-assembly of pyrene derivatives on Au(111): substituent effects on intermolecular interactions. *Chem. Commun.* **2014,** *50* (91), 14089-14092.
10. Wang, D.; Wan, L. J.; Xu, Q. M.; Wang, C.; Bai, C. L., Adlayer structures of pyrene and perylene on Cu(111): an in situ STM study. *Surface Science* **2001,** *478*.
11. Wan, L. J.; Itaya, K., In Situ Scanning Tunneling Microscopy of Benzene, Naphthalene, and Anthracene Adsorbed on Cu(111) in Solution. *Langmuir* **1997,** *13* (26), 7173-7179.
12. Yamada, T.; Shibuta, M.; Ami, Y.; Takano, Y.; Nonaka, A.; Miyakubo, K.; Munakata, T., Novel Growth of Naphthalene Overlayer on Cu(111) Studied by STM, LEED, and 2PPE. *J. Phy. Chem. C* **2010,** *114*, 13334-13339.
13. Kaposi, T.; Joshi, S.; Hoh, T.; Wiengarten, A.; Seufert, K.; Paszkiewicz, M.; Klappenberger, F.; Ecija, D.; Dordevic, L.; Marangoni, T.; Bonifazi, D.; Barth, J. V.; Auwarter, W., Supramolecular Spangling, Crocheting, and Knitting of Functionalized Pyrene Molecules on a Silver Surface. *ACS Nano* **2016,** *10* (8), 7665-7674.
14. Heckel, W.; Würger, T.; Müller, S.; Feldbauer, G., Van der Waals Interaction Really Matters: Energetics of Benzoic Acid on TiO_2 Rutile Surfaces. *J. Phys. Chem. C* **2017,** *121* (32), 17207-17214.
15. Heininger, C.; Kampschulte, L.; Wolfgang, M. H.; Lackinger, M., Distinct Differences in Self-Assembly of Aromatic Linear Dicarboxylic Acids. *Langmuir* **2009,** *25* (2), 968-972.
16. Pensa, E.; Albrecht, T., Controlling the Dynamic Instability of Capped Metal Nanoparticles on Metallic Surfaces. *J. Phys. Chem. Lett.* **2018,** *9* (1), 57-62.
17. Lelaidier, T.; Leoni, T.; Ranguis, A.; D'Aléo, A.; Fages, F.; Becker, C., Adsorption and Growth of Bis-pyrene Molecular Layers on Au(111) Studied by STM. *J. Phys. Chem. C* **2017,** *121* (13), 7214-7220.

18. Zuzak, R.; Dorel, R.; Krawiec, M.; Such, B.; Kolmer, M.; Szymonski, M.; Echavarren, A. M.; Godlewski, S., Nonacene Generated by On-Surface Dehydrogenation. *ACS Nano* **2017,** *11* (9), 9321-9329.
19. Pandurangachar, M.; Swamy, B. E.; Chandrashekar, B. N.; Gilbert, O.; Reddy, S.; Sherigara, B. S., Electrochemical Investigations of Potassium Ferricanide and Dopamine by 1-butyl-4-methylpyridinium tetrafluoro borate Modified Carbon Paste Electrode: A Cyclic Voltammetric Study. *Int. J. Electrochem. Sci.* **2010,** *5*, 1187-1202.
20. Rahman, M. M.; Jeon, I. C., Studies of Electrochemical Behavior of SWNT-film Electrodes. *J. Braz. Chem. Soc.* **2007,** *18*, 1150-1157.
21. Elgrishi, N.; Rountree, K. J.; McCarthy, B. D.; Rountree, E. S.; Eisenhart, T. T.; Dempsey, J. L., A Practical Beginner's Guide to Cyclic Voltammetry. *J. Chem. Educ.* **2017,** *95* (2), 197-206.
22. Adzic, R. R.; Zhang, J.; Sasaki, K.; Vukmirovic, M. B.; Shao, M.; Wang, J. X.; Nilekar, A. U.; Mavrikakis, M.; Valerio, J. A.; Uribe, F., Platinum Monolayer Fuel Cell Electrocatalysts. *Top. Catal.* **2007,** *46* (3-4), 249-262.
23. Vu, T.-H.; Wandlowski, T., Self-Assembled Structures of Benzoic Acid on Au(111) Surface. *Journal of Electronic Materials* **2017,** *46* (6), 3463-3471.
24. Vu, T.-H.; Wandlowski, T., CV and in situ STM study the adsorption behavior of benzoic acid at the electrified Au(100)| HClO4 interface: Structure and dynamics. *Journal of Electroanalytical Chemistry* **2016,** *776*, 40-48.
25. Kim, Y. G.; Yau, S. L.; Itaya, K., In Situ Scanning Tunneling Microscopy og Highly Ordered Adlayers of Aromatic Molecules on Well-Defined Pt(111) Electrodes in Solution: Benzoic Acid, Terephthalic Acid, and Pyrazine. *Langmuir* **1999,** *15*, 7810-7815.
26. Clair, S.; Pons, S.; Seitsonen, A. P.; Brune, H.; Kern, K.; Barth, J. V., STM study of terephthalic acid self-assembly on Au(111): Hydrogen-bonded sheets on an inhomogeneous substrate. *J. Phys. Chem. B* **2004,** *108*, 14585-14590.
27. Lu, J.; Zeng, Q.; Wang, C.; Zheng, Q.; Wan, L.; Bai, C., Self-assembled two-dimensional hexagonal networks. *J. Mater. Chem.* **2002,** *12* (10), 2856-2858.
28. Vogt, M. R.; Nichols, R. J.; Magnussen, O. M.; Behm, R. J., Benzotriazole Adsorption and Inhibition of Cu(100) Corrosion in HCl: A Combined in Situ STM and in Situ FTIR Spectroscopy Study. *J. Phy. Chem. B* **1998,** *102*, 5859-5865.
29. Bonello, J. M.; Williams, F. J.; Lambert, R. M., Aspects of Enantioselective Heterogeneous Catalysis: Structure and Reactivity of (S)-(-)-1-(1-Naphthyl)ethylamine on Pt{111}. *J. Am. Chem. Soc.* **2003,** *125* (9).
30. Mandler, D.; Kraus-Ophir, S., Self-assembled monolayers (SAMs) for electrochemical sensing. *J. Solid State Electrochem.* **2011,** *15* (7-8), 1535-1558.
31. Chang, Y.; Tang, N.; Qu, H.; Liu, J.; Zhang, D.; Zhang, H.; Pang, W.; Duan, X., Detection of Volatile Organic Compounds by Self-assembled Monolayer Coated Sensor Array with Concentration-independent Fingerprints. *Sci. Rep.* **2016,** *6*.
32. Skomski, D.; Tempas, C. D.; Cook, B. J.; Polezhaev, A. V.; Smith, K. A.; Caulton, K. G.; Tait, S. L., Two- and Three-Electron Oxidation of Single-Site Vanadium Centers at Surfaces by Ligand Design. *J. Am. Chem. Soc.* **2015,** *137* (24), 7898-7902.
33. Williams, C. G.; Wang, M.; Skomski, D.; Tempas, C. D.; Kesmodel, L. L.; Tait, S. L., Dehydrocyclization of peripheral alkyl groups in porphyrins at Cu(100) and Ag(111) surfaces. *Surface Science* **2016,** *653*, 130-137.
34. Afsari, S.; Li, Z.; Borguet, E., Orientation-controlled single-molecule junctions. *Angew Chem Int Ed Engl* **2014,** *53* (37), 9771-9774.

CHAPTER 2: INSTRUMENTAL WORKING PRINCIPLE AND METHOD

2.1: STM WORKING PRINCIPLE

2.1.1: GENERAL STM

One of the major tools used throughout this project is a Molecular Imaging Microscope (Agilent/Keysight) for the purpose of using Scanning Tunneling Microscopic (STM) techniques to develop observations of adsorbed adlayers on a substrate and the solutions' cyclic voltammograms. Where STM involves at least four electrodes, the STM probe (the tip), the Working Electrode (WE, understood as the substrate), the Reference Electrode (RE, Pt wire), and the Counter Electrode (CE, Pt wire). This technique produces images with atomic resolution, which requires that the tip be extremely sharp, theoretically, one atom at the apex of the tip. This super sharp tip is placed inside the STM scanner, which holds the three-dimensional Piezoelectric Material (PEM). The PEM is a solid material that when stressed with compression or elongation an electric field is produced, or, when an electric field is applied to the solid material, it will either compress or elongate in the nanometer (nm) scale. This is controlled by the PicoView software and helps with producing images by moving the tip, fractions of a nm at a time over the substrate.

Another purpose of the PEM is to move the tip in the nm scale in the x-, y-, and/or z-direction for scanning the substrate so that an image can developed. However, the purpose of obtaining an extremely small distance between the tip and substrate is an imperative hurtle to overcome. Luckily, this instrument and its software makes this hurtle relatively easy to overcome. The software parameter, Stop At (%), is set by the user so that the automated approach will be stopped before the tip crashes into the substrate. This parameter is the percentage of signal measured, due to quantum tunneling, with respect to the signal that would be present if the electrodes were connected. The PEM will move the tip as far as it can go, if no signal is measured

or if the measured signal percentage is less than the Stop At parameter during this process, then the tip will be retracted and the sample will mechanically move closer to the tip and the process will begin again as a loop, while constantly measuring for the Stop At signal. This loop will continue to reduce the distance between the tip and the substrate (tip-substrate distance) until the Stop At parameter is equal to the measured signal percentage, which halts the approach and the distance between the tip and substrate is extremely small.

Additionally, two other parameters that are controlled by the user, are the potential that is applied to the tip and the potential that is applied to the substrate (E_S). Where the difference between the two potentials is referred to as the potential bias. The two potentials need to be different for the current (produced from electrons tunneling between the substrate and the tip) to be measured, that is the potential difference cannot equal zero, otherwise no current will be measured. Quantum tunneling allows for imaging to be possible, where quantum tunneling is more formally and generally known as a particle overcoming an energy barrier that is classically forbidden. In this case, the particle is an electron while the energy barrier is the tip-substrate distance that the electron travels. The tip-substrate distance is roughly 1-2nm and when enough electrons transfer, a current is produced, known as the tunneling current. This tunneling current is measured by the instrument and depending on the scanning mode, the changes in the tip-substrate distance or tunneling current are recorded as the tip scans over the substrate. The relationship between the Tunneling Current (I_t), Potential Bias (E_{bias}), and tip-substrate distance (s) is found as the proportionality equation in Figure 2.1.

$Proportionality\ Equation:\ I_T \propto E_{bias} e^{(-ks\sqrt{\Phi})}$		
$X \uparrow \equiv X\ value\ increases$	$Direct\ Proportionality$	$Inverse\ Proportionality$
$X \downarrow \equiv X\ value\ increases$	$E_{bias} \uparrow Then\ I_T \uparrow$	$I_T \uparrow Then\ s \downarrow$
$X = I_T, E_{bias}, or\ s$	$E_{bias} \downarrow Then\ I_T \downarrow$	$I_T \downarrow Then\ s \uparrow$

Figure 2.1: This figure presents the proportionality equation and the relationships between specific variables.

*The PE is a common concept that describes how STM produces signal for measurements.[1]

The Proportionality Equation (PE) in Figure 2.1 helps with interpreting an image, however, must be used in combination with the knowledge of the scanning mode to discern image features. There are two types of scanning modes utilized within the STM software, they are constant height and constant current scanning modes. The constant height scanning mode sets the tip-substrate distance to be fixed as it scans over the substrate. While scanning the substrate's surface in this mode, the tunneling current will change, and these changes are recorded and converted to an image. Whereas, the constant current scanning mode sets the tunneling current to be fixed by changing the tip-substrate distance. That is, as the tip scans over an area that produces an increase in tunneling current, the tip-substrate distance increases, similarly, if the tip scans over an area that produces a decrease in tunneling current, the tip-substrate distance decreases, as Figure 2.1 illustrates. The changes in the tip-substrate distance are recorded and converted as an image in this constant current mode.

The changes in either tunneling current or height (depending on scanning mode) are seen in the converted images as brighter or darker areas (or alternating colors, depending on software) corresponding to atoms, spaces between atoms, and/or features of the substrate/adsorbates. The images that are produced by either scanning mode are dictated by the geometric and electronic

features of the substrate/adsorbates. The geometric contribution to the image can be found as the topographical surface features of the substrate (e.g. terraces at different heights), arrangement of atoms on the substrate surface (e.g. Miller Indices (111) or (100)), and/or the way adsorbates adsorb onto the substrate's surface (e.g. an ordered or disordered adlayer). Whereas, the electronic contribution of the image relates more to the conductivity of the substrate, adsorbates, or the substrate-adsorbates interaction. Yet, both contributions are present in each image produced by STM, where the combination of the PE in Figure 2.1, the scanning mode, and the types of contributions assist in the interpretation of surface features.

Alternatively, good procedural experimentation calls for the constant vigilance against contamination (for solutions and equipment), improper equipment (such as dull or poorly coated STM probes), and/or the instability/vibration of the instrumental apparatus (allows for drift). Where contamination/cleanliness of solutions and equipment will be covered in Chapter 4 and STM probe sharpness/coating will be covered in Chapter 3. However, to eliminate vibration and increase in the instrumental apparatus stability, is relatively easy due to a simple strategy found in the experimental procedure. The equipment that holds the apparatus helps with this issue where the STM probe and scanner is placed, sits on a platform with vibration dampener feet, that reduce the amount of vibration. Additionally, the platform hangs from inside the Faraday box by bungy cords that also reduce vibration, also, the Faraday box sits on a table that has vibration dampeners in between the legs of the table and the table top, which helps reduce vibration, see Figure 2.2.

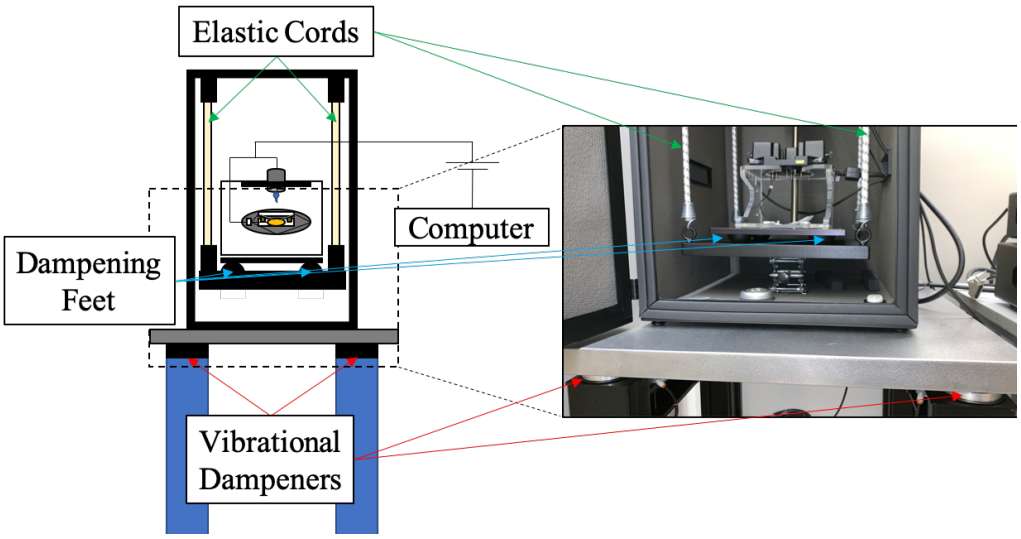

Figure 2.2: PowerPoint drawing of the STM probe and scanner in circuit with the actual apparatus.

This three-tiered vibration reduction system helps a great deal, however, if the individual is not careful and strategic with their experimental procedure then they might end up being counterproductive by introducing vibration. Within the STM procedure there are three sections that include instrument preparation, sample preparation, and instrumentation. Where instrument preparation and sample preparation will be covered in Chapter 4. Instrumentation will cover from the point where the sample has been prepared and placed in the instrument, where after this point, there has to be a sample to tip approach (referred to as the approach) to get the tip extremely close to the substrate so that images can be developed. However, approaching the sample can introduce small amounts of vibration.

Additionally, trying to image the same day the STM probe and scanner is placed in the STM apparatus adds significant vibration and causes the "drift" of the STM tip, i.e., the position of the STM tip constantly changes with time, making the imaging of a specific area impossible. These two things can affect the images in a negative manner, thus, to reduce the vibration from introducing the equipment can be done by letting the instrument sit overnight after the STM

scanner with the tip has been integrated into the apparatus. To reduce the vibration coming from the approach can be done by approaching the sample to tip at a slow rate and stopping every 20 Micrometers (μm) to let the system stabilize. Once the approach stops (by the Stop At parameter), withdrawing the tip and sample (referred to as the withdraw) by roughly ten μm, then re-approaching at the slowest rate that the software will allow and wait thirty minutes to an hour before imaging (so long as the piezo bar is stable, will be covered in Chapter 4).

2.1.2: TYPES OF STM TECHNIQUES/CONDITIONS

Even though STM is a type of technique within Scanning Probe Microscopy (SPM), STM can be further understood through the three types of techniques or conditions of STM, all of which require conductivity. These three techniques are ambient (in-air), UHV, and EC STM. Where ambient and UHV STM are most often used in the study of solid-vapor (gas) interfaces, and EC-STM is used for the study of solid-liquid interfaces. Each technique or condition of STM has its set of requirements to function properly. For example, ambient and UHV STM requires a super sharp tip (does not need to be coated with an insulating material) and the working electrode. Whereas, EC-STM requires the super sharp tip that has been coated with an insulating material, the working electrode, an electrolyte solution, a CE, and a RE.

The requirement of having a working, reference, and counter electrode is normal throughout electrochemical experiments and measurements. However, EC-STM, requires a fourth electrode, the STM tip. Where, under EC-STM, it is required that the tip be coated with an insulating material to reduce the amount of leaking current from the STM tip, so that a discernable image can be developed. This is consequential to the fact that there is a length of the tip that will be exposed to the electrolyte solution that sits on top of the substrate and the tip being 1-2 nm from the surface of the substrate. If there was not an insulating layer around the majority of the tip, then

the current applied to the tip would leak out into the electrolyte solution, creating a lot of noise that will be overlapped with the signal from the substrate. However, if all the surface area of the tip that would be exposed to the electrolyte solution was coated with an insulating material, except the apex of the tip, then noise will be dramatically reduced while the signal will be most dominant. The apex of the tip needs to be exposed in order to measure the signal from the substrate, see Figure 2.3.

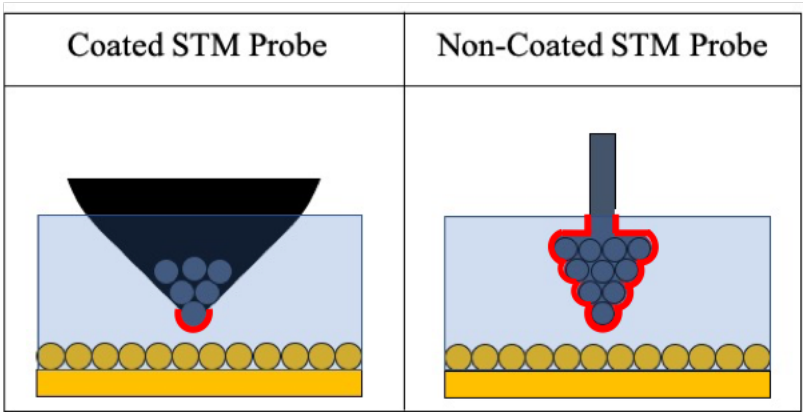

Figure 2.3: PowerPoint drawing of Coated and Non-coated (bare) STM probes exposure to electrolyte solution (outlined in red).

2.2: ELECTROCHEMISTRY

2.2.1: CYCLIC VOLTAMMETRY

EC-STM offers another insightful tool in combination with this STM technique, which is CV, where traditionally, this technique is used to study electrochemical reactions such as redox reactions potentials' (Faradaic processes). Instead, for this project, the non-Faradaic (adsorption/desorption) processes that occurs will be studied, in a potential range to prevent the oxidation or reduction of the electrodes and electrolyte solution, yet, CV still offers more information to be retrieved from the limited potential experiments. That is, STM can offer information on what the molecule-molecule and molecule-substrate interactions might be for a

given adsorption phase. However, a CV shows the potential regions (that an adsorption phase can be explored by EC-STM imaging), separated by Adsorption/Desorption (A/D) Peaks ($P_{A/D}$). This can be thought of as an interpretation of a map, where an A/D peak is the location of a border between two regions in space and the potential region between two peaks represents only one region (see Figure 2.4).

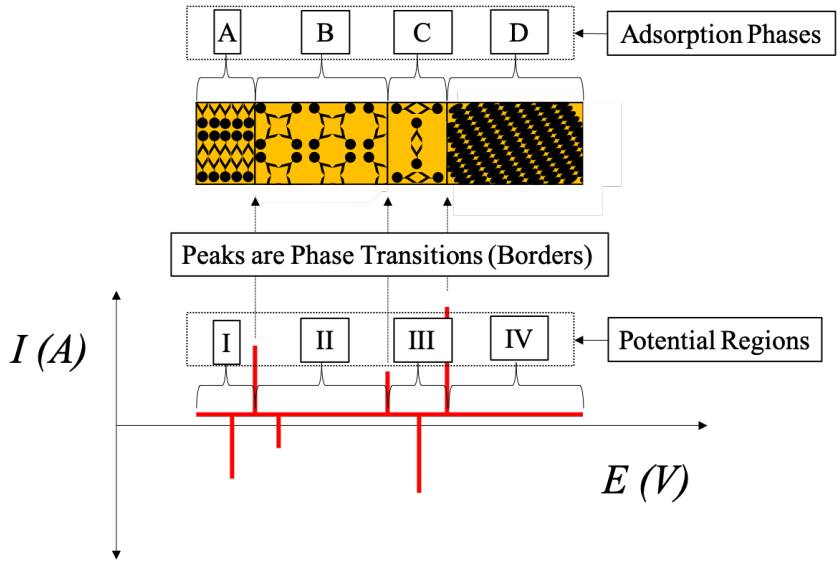

Figure 2.4: Non-Faradaic CV PowerPoint drawing showing the physical meaning of peaks and regions in between peaks.

These peaks are the transitions between A/D phases and can be measured in a cathodic or anodic potential sweep, that is in a positive potential direction or in a negative potential direction, respectively. Where the location of the cathodic and anodic peaks can change locations with respect to the potential based on convention. The convention of reporting CV data according to IUPAC regulations is to plot CVs as Current vs. Potential, with the low potential on the left and high potentials on the right of the x-axis (whereas the x-axis is flipped for US convention).[2]

The A/D peaks can be influenced by various parameters, such as, scan rate, electrodes' materials, electrode features, electrolyte solution, and molecules dissolved in the electrolyte

solution (sample solution). Where the focus of non-Faradaic processes and the three parameters (electrodes' materials, electrolyte solution, and sample solution) limit the potential window for experiments. However, the type of equipment used for the experiments should be relatively (chemically and electrochemically) inert. That is when the electrodes are exposed to the electrolyte solution or the sample solution there should not be a reaction occurring and within the potential window there should not be any charge transfer reactions occurring. Fortunately, most electrodes are noble metals and should not react with the solutions and their redox potentials are outside of the potential window, to ensure no Faradaic processes occur.

Throughout this project, 0.6 mm Pt wires are used as the quasi-reference and counter electrodes. These Pt wires are very inert and do not chemically react and are resistant to electrochemical etching. However, they are also convenient to work with, regarding to the cleaning (flame annealing) and flexibility (shaping and moving to work in an electrochemical cell) of the Pt wires. The low surface area of the CE (Pt-wire), RE (Pt-wire), and WE (Au-disk) with the low current that flows throughout the cell helps with reducing the ohmic drop to the point where it is negligible. Another helpful method of minimizing the ohmic drop is to reduce the distance between the RE and the WE, which is done in each experiment.

2.2.2: A/D PEAKS

The A/D peaks help to understand how many different ways the molecules and/or ionic species in solution may be adsorbing on the substrate, known as phases. However, the goal is to observe, with atomic resolution under EC-STM conditions, the long-range ordered nanostructures that are formed from the potential induced adsorbed molecules. These long-range ordered nanostructures can be seen as patterns, due to their repetitive features. Dissimilarly, the adsorption of the molecules and/or ionic species that form non-pattern or non-long-range ordered

nanostructures are defined as disordered adlayers. It is quite difficult to get atomic resolution of these disordered adlayers, and as a result, no information on the molecule-molecule and molecule-substrate interactions can be determined from the STM images alone. The CV may have regions of both ordered and disordered phases; however, they are directly observed with STM.

When observing the different phase patterns in a CV, it should be known that the current is a function of potential. As a result, by changing the value of the E_s, it could also change the adsorption patterns observed; for example, if the E_s is set to a value that is found in between set of adjacent peaks. Where, again, each peak is representative of a phase transition and the space between peaks are representative of a specific adsorption phase. That is, if the E_s is equal to the potential where the peak apex is found, then a co-existence of different patterns might be observed. The individual patterns should be first observed, and the information understood before understanding the co-existence of the different phases, although the rate at which the phase transition and how the different phases interact would be interesting yet difficult avenues to study.

2.3: STM PROBE

2.3.1: TUNGSTEN WIRE EXPOSED TO AIR

Throughout this project, the probes used for the experiments are made from 0.25 mm W wires. However, the development of these probes will be discussed further in chapter 3, yet, it should be noted that the material, Tungsten (W), will be oxidized when exposed to air for long periods of time. Additionally, after the W-tips have been developed, they cannot be used for many experiments. In fact, it is quite discouraged that the same probe is used for more than three experiments. This is because even the best W-tip that has been developed has an “expiration date” that will affect the resolution of the images or prevent the ability to image. This expiration date is due to the oxidation of the exposed W-tip surface to the air, alternatively, the use of W-tip with

imaging dulls the apex of the tip which reduces the resolution of the images, that could prevent atomic resolution.

2.3.2: THE DULLING OF AN STM PROBE APEX

As the tip scans the substrate or adsorbates, the interactions may alter the apex of the tip. That is, the constant interaction and scanning of the tip along the substrate's surface can cause defects in the tip apex. Over time, or after two to three experiments, the images might show that the tip becomes dull, which is seen in the image by the lack of distinguishability between the terraces of the substrate that are at different heights or the lack of atomic resolution. If the tip is sharp, the difference between the terraces is readily seen by a sharp line that separates one lighter shaded terrace (the higher terrace) and the darker shaded terrace (the lower terrace), see Figure 2.5. As the tip dulls or if the tip is dull to begin with then the line that separates the two terraces will not be readily seen instead it will appear as a gradual change from one height to the other.

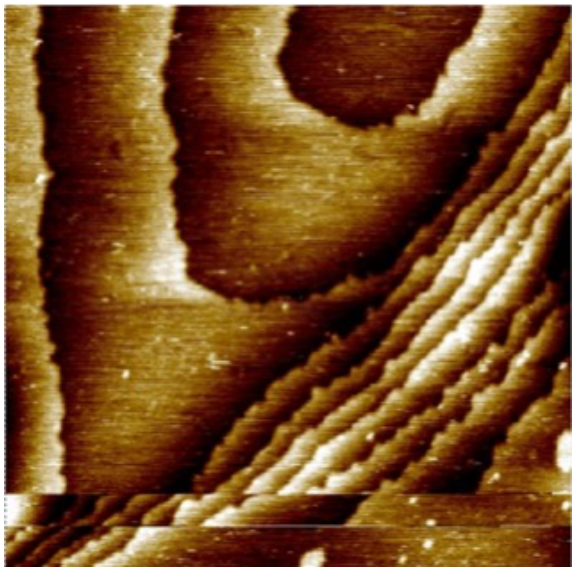

Figure 2.5: 200 x 200 nm image of the Au crystal in 0.05 M H_2SO_4 E_S = -314 mV. This image is used to show how relatively sharp the lines between terraces can be seen if the STM probe is also very sharp.

2.3.3: THE LEAKING CURRENT/NOISE

The tip coating helps to reduce the amount of leaking current; however, it will not completely remove the leaking current. If it does, then, none of the tip is exposed to the electrolyte solution and no signal can be measured, which will result in not being able to develop an image and provides the possibility of damaging the tip and the substrate. However, over each experiment, it can be found that the leaking current will increase. This is due to the electrolyte solution that slowly breaks apart the dried wax, exposing more wire to the electrolyte solution, which increases the leaking current. Rinsing the tip with water to remove electrolyte on it between each use helps prevent the coating damage, however, does not stop it entirely. This is because the coating is damaged while the tip is being used to make measurements where it is exposed to the electrolyte solution. As a result, after two or three uses, the leaking current climbs so high that resolution is lowered or might even prevent the ability to image by a buildup of noise overlapping with the measured signal.

2.4: CHAPTER TWO REFERENCES

1. Pobelov, I. V. Electron Transport Studies - An Electrochemical Scanning Tunneling Microscopy Approach. Saransk, Republic of Mordovia, 2008.
2. Elgrishi, N.; Rountree, K. J.; McCarthy, B. D.; Rountree, E. S.; Eisenhart, T. T.; Dempsey, J. L., A Practical Beginner's Guide to Cyclic Voltammetry. *J. Chem. Educ.* **2017,** *95* (2), 197-206.

CHAPTER 3: DEVELOPMENT OF STM PROBE FABRICATION TECHNIQUES

3.1: STM PROBE MATERIAL

There are many types of tips used for STM, however, what determines the tip material that should be used is based on the ability of making the probes super sharp, the convenience of making the probes super sharp, the requirements of the probe, and the potential window of the experiment. There are at least two ways of making STM super sharp tips, these two ways are EC-etching and mechanical sharpening thin wires composed of the probe material. However, the requirements of STM tips are that they have to be super sharp, the material must be conductive, the material should be very inert and depending on the experimental parameters, the tip should not undergo a charge transfer reaction (Faradaic process) while being exposed to the electrolyte solution (control or sample solution) and having a potential applied to it. Ideally, the STM tip should be an Ideal Polarized Electrode (IPE). An IPE is an electrode that will not undergo a Faradaic process with the electrolyte solution that surrounds the probe within a potential window for study, no matter how much potential is applied to it.

Unfortunately, not all of the requirements can be met, for example, Platinum/Iridium (Pt/Ir) alloy is often the material for the probes used throughout STM experiments and is very inert. Yet, for the purpose of developing STM tips, the sharpening technique for this material is done by mechanical sharpening, which is not the technique chosen for this work because of how inefficient it is in comparison with the EC-etching technique. Instead, Pt/Ir wires are used for charge transfer reactions, e.g. EC-etching W wires. Pt/Ir is one of the best tip materials to use because of how inert it is, yet this noble metal alloy is quite expensive in comparison to W. W is the probe of choice throughout this project because of the convenience and efficiency producing the probes by EC-

etching and that the EC-etching process does not include hazardous byproducts, like that of EC-etching Pt/Ir wires.[1-3]

The previous two examples, Pt/Ir and W are common materials used for STM tips, however, another common material used for STM tips is that of Au wires. Where Au wires are more expensive than W wires, but not to the extent of the Pt/Ir wires cost. However, Au has not been used for the purpose of this project, which is due to the fact that EC-etching of a gold wire to produce a super sharp tip is challenging and produces toxic gas (chlorine gas).[4] The gold tip fabricated by EC-etching is usually not as sharp as an EC-etched W tip. Additionally, substrate material in this project is also gold – Au(111). This might be a problem for the STM experiment, that is having the same material for the STM probe and substrate, because this could promote the adsorption of molecules onto the tip (if there is enough surface area of the tip exposed to the electrolyte solution) which would cause interference with the development of the STM images.

3.2: PRODUCING SUPER SHARP STM PROBES

3.2.1: EC-ETCHING VS. MECHANICALLY SHARPENING PROBES

The EC-etching technique is not something new or novel with this work, instead, optimizing this type of method has been attempted in this work, e.g. the EC-etching of W wires.[2, 5-6] Using EC-etching techniques with W tips have shown to be the easiest route to obtain super sharp STM probes. One can use Pt/Ir wire with a mechanical sharpening technique; this requires a cutting and pulling method that often produces dull or jagged apexes that cannot be used for experimentation. This process involves simultaneously cutting and pulling a Pt/Ir wire in a quick, angled, jerking motion with a sharp pair of scissors. This technique might produce a somewhat sharp tip; however, it takes quite some time to get used to the technique to efficiently produce

super sharp tips. Unless plenty of practice and experience is placed in this technique, it is often the case that the apex is not very sharp, and one must repeat the sharpening attempts.

However, it is quite easier to produce super sharp W tips by EC-etching W wires. Where the EC-etching process involves a Direct Current (DC) power supply that allows for a positive lead to connect to the W wire (the anode) and a negative lead that connects to the Pt/Ir wire (the cathode), which is in the shape of a ring with a tail to connect to the lead. This process also involves the electrolyte solution that allows the etching of the W wire to take place. Which is technique is simple in comparison, because, all that needs to be done is setting the potential for the reaction to take place at a certain rate, use the electrolyte solution to connect the anode to the cathode, and apply the potential to the circuit until the etching is finished. As soon as the etching process is finished, it is imperative that the power supply is switched off to prevent any extra (unwanted) etching to occur. The extra etching could dull the apex of the developed tip and produce an image like Figure 3.1.

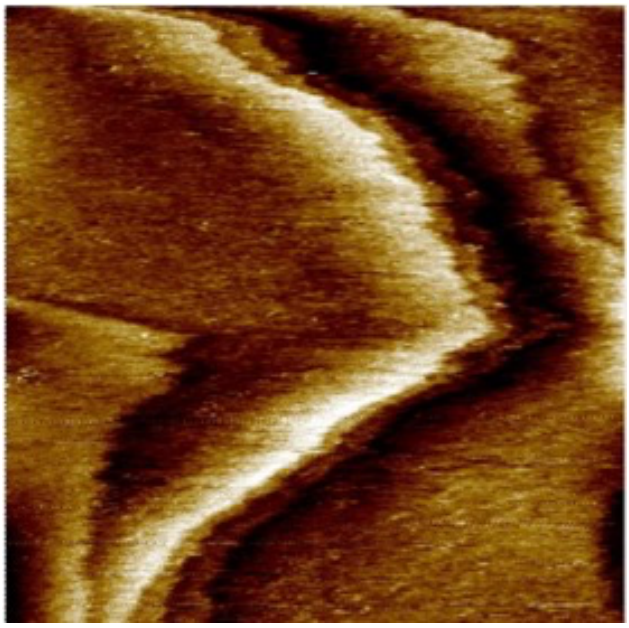

Figure 3.1: 50x50 nm image of the Au crystal in 0.05 M H_2SO_4 E_S = -200 mV. This image is used to show how relatively wide the lines between terraces can be seen if the STM probe is relatively dull.

3.2.2: EC-ETCHING PRINCIPLE, PROCEDURE, AND METHODS

3.2.2.1: EC-ETCHING PRINCIPLE

The electrolyte solution, used to etch the W wire, is 2 M NaOH. This solution completes the circuit that allows the reaction to occur after the potential is set and applied. The process of etching the solid wire is an oxidation reaction that produces Na_2WO_4 which is soluble in water.[1]

$$W(s) + 2NaOH(aq) + 2H_2O(l) \rightarrow Na_2WO_4(aq) + 3H_2(g)$$

Figure 3.2: Known reaction for the EC-etching of W wire into an STM probe.[5]

As the etching occurs, the outer layer, exposed to the electrolyte solution, is etched away, where the 0.25 mm wire becomes significantly thinner as the potential is applied over time. As the wire is thinned, the bottom portion of the wire is pulled by the gravitational force of its mass, which stretches the wire, see Figure 3.3. Eventually the wire, that is exposed to the electrolyte solution will be completely etched away, however, the thinned part will get so thin and will be pulled enough by gravity that the two portions will break. After the break of the two portions, it is probable that at least one usable super sharp tip will be developed. Once the tip breaks, it is imperative that the power supply should be shut off or the circuit must be broken right away. If one of these options do not occur right away, then the etching reaction will continue which will dull the apex of the tip, dulling the tip.

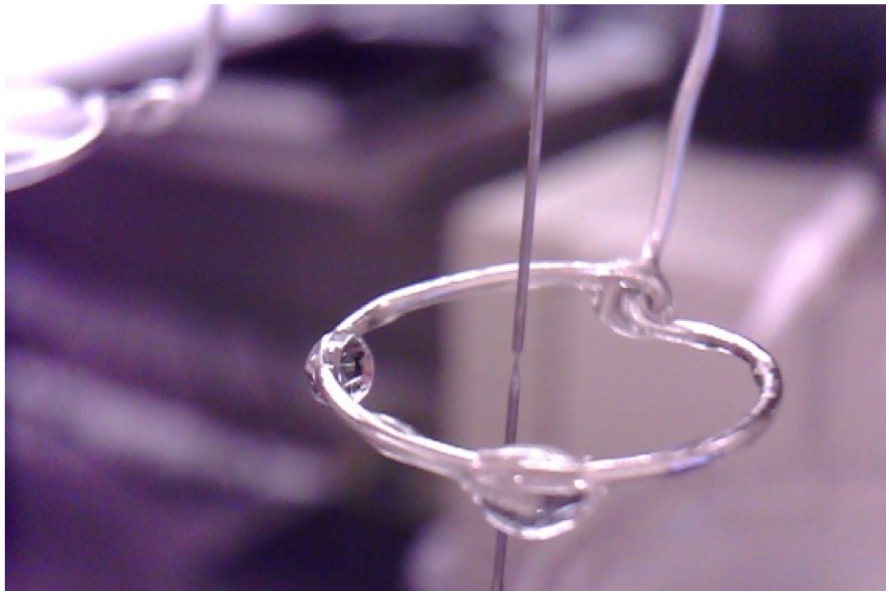

Figure 3.3: EC-etching of a W wire where the 2 M NaOH film was broken after only a few minutes at an applied potential of 2.7V (according to the direct current power supply).

3.2.2.2: EC-ETCHING PROCEDURE

Setting up the EC-etching apparatus involves, preparing and connecting the W wire, preparing the Pt/Ir cathode, setting the potential parameter, connecting the electrodes with the electrolyte solution, and (depending on EC-etching method) placing a rubber cork-well underneath the bottom half of the W wire. Where preparing the Pt/Ir wire is just forming the electrode shape into a ring with a tail to connect it to the cathode lead and rinsing it with water to clean the electrode. However, preparing the W wire involves cutting the W wire to the length of 3.5-4.0 mm and then straightening the wire as much as possible with tweezers, then connecting the W wire to the anode lead. Connecting the electrodes by the electrolyte solution can be done differently, depending on the EC-etching method.

Once both electrodes are prepared, the apparatus is completely set up, and the power supply is on, then waiting until completion of the reaction is the only necessary action. One must watch the bottom portion of the tip so that as soon as it breaks off (and caught by the rubber cork-well),

the power supply is turned off and the electrolyte solution is removed or, vice versa, so long as the actions are quick. Then rinsing the tip with water to remove the etching solution that remains on the tip, afterwards, the tip can be used for the coating process or stored in secure area to ensure the safety of the tip. Then repeating this procedure is necessary to produce many tips, because not all the tips that are EC-etched will be sharp enough to be used for STM imaging. The goal is to produce as many super sharp tips as possible in a given amount of time and use the best two or three for the STM imaging experiment.

3.2.2.3: EC-ETCHING METHODS

One of the three following EC-etching methods was chosen based on what best produces the STM probes: Method 1, Method 2, and Method 3. Where the sharper the tip, the better, however, the other goal was to develop as many super sharp tips as possible in one day so that the process of choosing a tip to be used for an experiment can be very selective. When a tip is thought to be sharp, the probe will have a small/short apex when looking at it under an optical microscope. However, this does not give a true qualitative idea on how sharp the tip might be. A true qualitative test would be to use the tip when trying to image and finding an area that has a terrace where one area is at a different height than the other and where these two regions meet are separated by are sharp thin line like in Figure 2.5. Whereas, a dulled tip would not produce a sharp separation line, instead, a gradual change from lower/higher area to the other higher/lower area. Alternatively, the apparatus used for the three methods is the same as the apparatus found in Figure 3.4.

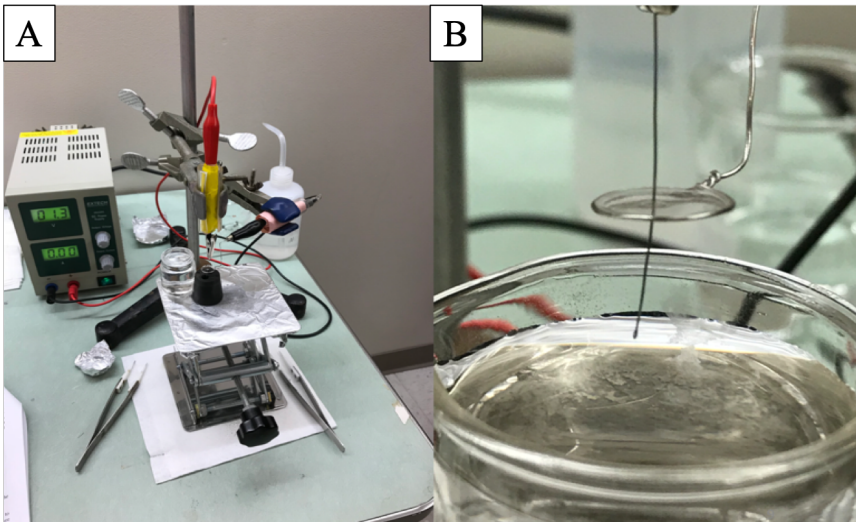

Figure 3.4: Old EC-etching apparatus, where only one Pt ring is used and a small rubber cork with a small hole drilled out to catch the probe as the bottom half of the W wire brakes off (A). (B) is a zoomed in where the electrolyte solution is seen as a thin film around the W wire.

Method 1 consists of a beaker of 2 M NaOH solution with the Pt/Ir cathode is submerged, anywhere in the electrolyte solution. Whereas, the W anode is placed only a few Millimeters (mm) into the solution. As the DC power supply forces the etching reaction to occur, the bottom portion of the W wire will thin and break off. The result of this method is the production of one possibly super sharp tip, which is the portion of the wire that did not break off. This method is very common and is seen of multiple sources for literature.[1, 6] Please refer to Figure 3.5.

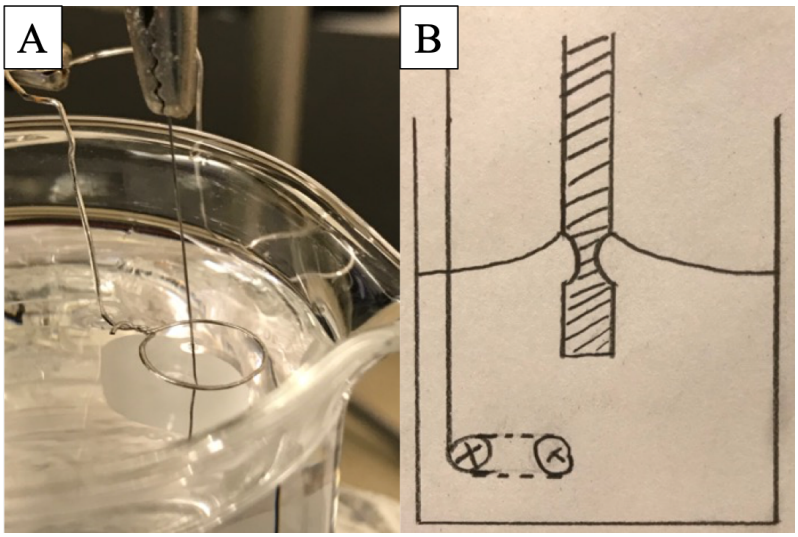

Figure 3.5: (A) is the what the EC-etching Method 1 would look like in practice and (B) is a drawing of the cross section of the solution as the etching is taken place.

Method 2 consists of the Pt/Ir cathode ring and the W wire placed in the center of the ring (perpendicular to the plane of the ring) and the plane of the ring is at half of the length of the W wire. Then the beaker of 2 M NaOH solution is used to submerge both electrodes until the Pt/Ir ring is completely covered by the solution. The solution is then removed allowing for a thin film to stay inside the ring of the Pt/Ir ring, surrounding the W wire. As the DC power supply forces the etching reaction to occur, the bottom half of the W wire will break off and be caught by rubber stopper with the rubber cork-well. The result of this method is the production of two possibly super sharp tips. This method had been studied well such that it is understood that the bottom half of the W wire that breaks off as an STM probe is quite sharp.[7] Please refer to Figure 3.6.

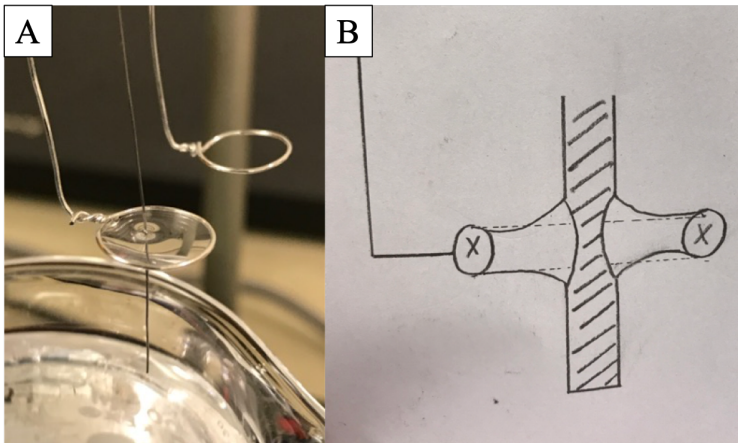

Figure 3.6: (A) is the what the EC-etching Method 2 would look like in practice and (B) is a drawing of the cross section of the solution as the etching is taken place.

Method 3 is somewhat of a combination between Method 1 and Method 2, where the electrode set up is the similar to Method 2, except the plane of the Pt/Ir ring is not at half of the length of the W wire. Instead the plane intersects a few mm before the end of the W wire. The electrodes are submerged in the 2 M NaOH solution until the Pt/Ir ring is completely submerged. Then the solution is lowered, or the electrodes are raised such that the Pt/Ir ring is just above the level of 2 M NaOH solution in the beaker, yet that solution coheres to the Pt/Ir ring and W wire in a parabolic bend between the two electrodes. As the DC power supply forces the etching reaction to occur, the bottom portion of the W wire will break off. The result of this method is the production of one possibly super sharp tip. This method is thought to help with controlling the shape of the probe apex due to the way the electrolyte solution coheres to the electrodes. Please refer to Figure 3.7.

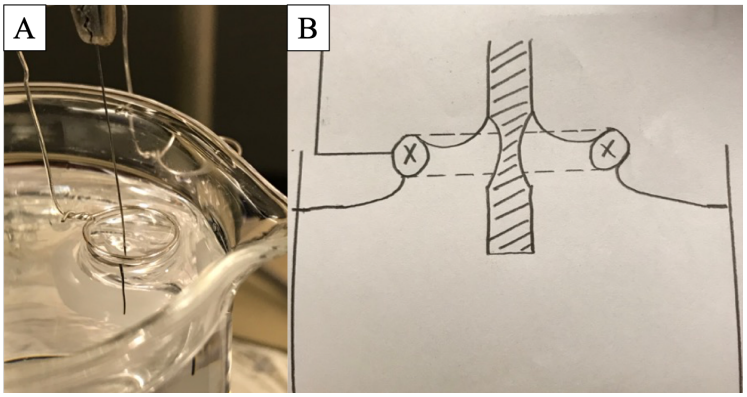

Figure 3.7: (A) is the what the EC-etching Method 3 would look like in practice and (B) is a drawing of the cross section of the solution as the etching is taken place.

From the literature and the practice of these three methods, it was found that the shape of the electrodes was not easily controlled, in fact, it was very inconsistent in shape from one etching attempt to another. Yet for all methods, even though the shape of the probe varied, they still appeared sharp when observing them under an optical microscope for each etching method, despite the different shapes. However, Method 2 produced twice as many tips as Method 1 or Method 3. This, in the end, help increase the chances of producing multiple super sharp tips. Also, for method 2, when the lower part of W wire (lower top or bottom half) breaks off, the electrolyte film often breaks too, so that the EC-etching reaction stops immediately. Even if the electrolyte film does not break, the continued EC-etching only can dull the upper tip (top half), not the lower one because the lower tip would have already broken off and dropped into the cork-well. But for the method 1 and 3, there is a risk that the EC-etching will continue to etch away (dull) the tip apex. The tips' sharpness from method 2 were quantified by the following TEM data in Figure 3.8.

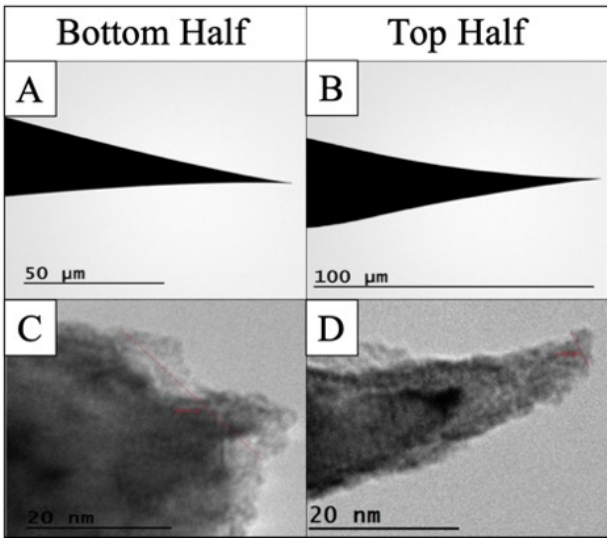

Figure 3.8: TEM images of the top and bottom half of an EC-etched W wire. Where the diameter of the apex for the top half was roughly 5 nm and the bottom half was roughly 30 nm.

In Figure 3.7 it can be seen that relative apex of each tip, top and bottom half, is very sharp. Where the top half has an apex diameter at roughly 30 nm, and the lower half has an apex diameter at roughly 5nm. However, these tips could not be used for STM experiments after measured with TEM, because, in order to measure the tips with TEM the EC-etched tips had to be cut to such short lengths that they would not fit inside the STM scanner. Thus, one can conclude that the tips made from this method are of similar sharpness. Yet, even though the sharpness cannot be measured before each STM experiment, the STM experiment will show a relatively qualitative sharpness for the tip in use for the experiment from method 2. However, there is another method that was not explored that might be of interest, yet seems rather difficult which is where Hobara et al. introduced a dynamic etching process of method 1 rather than the static etching process (where the W wire is stationary).[8]

3.3: COATING PROBES

3.3.1: COATING PRINCIPLE

Coating the STM probe is an essential requirement of all EC-STM experiments. This is due to the nature of the experiments held at the solid-liquid interface, which, is the electrode-electrolyte interface with respect to the experiments in this work. Where the more surface area of the bare W probe that is exposed to the electrolyte solution the greater the leaking current (noise) will be, however, there has to be some surface area of the apex of the tip exposed to the solution to allow quantum tunneling to occur so that imaging might be possible. If there is too much of the tip exposed, then the leaking current will overlap and, if strong enough, then it will completely mask the tunneling current (signal) which will prevent the tip from getting close enough to the substrate for quantum tunneling to occur and be observed (within 1-2 nm from the substrate). As a result, no discernable images will be developed.

Alternatively, one has to be careful not to coat the entire apex of the probe so that imaging can be made possible and to ensure the safety of the probe and the substrate, see Figure 3.9 for an example of etched and coated W probes.

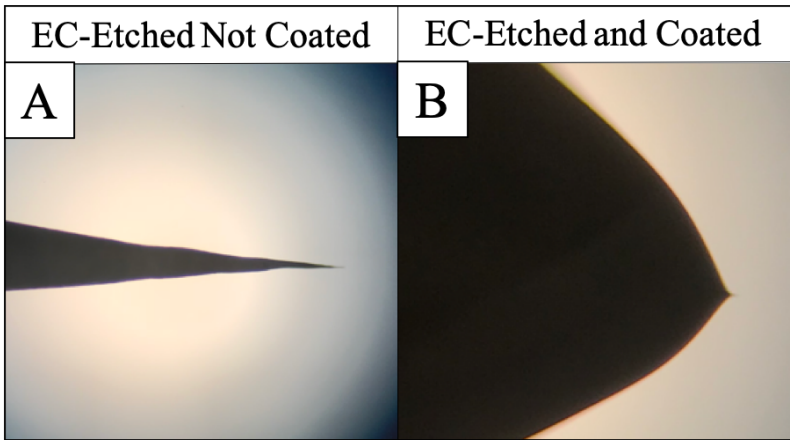

Figure 3.9: These images show the visual difference between an STM EC-etched probe without coating (A) and after coated with Apiezon wax (B) under an optical microscope.

The EC-Cell holds roughly 0.3 mL electrolyte that stands in the cell-well at a height of roughly 4 mm, which means that the tip should have a coated length of 4mm or greater. Thus, all tips that have been coated are in the range of 5-9 mm in coating length, see Figure 3.10 for examples of the coating length.

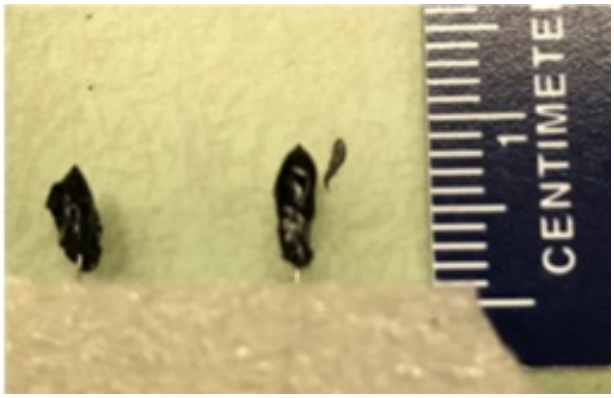

Figure 3.10: Finished probes produced from W wires that have been EC-etched and coated with Apiezon wax where it can be seen that the length of the coating layer is roughly 5-7 mm.

3.3.2: COATING MATERIAL

The coating material, like the EC-etching process, has its own set of requirements which are that the coating material has relatively low boiling point, that the material is an insulator, that the material is insoluble in the electrolyte solution, and is clean. Thus, there are a few options that can meet most if not all of these requirements, a few of them are nail polish[9], polyethylene[10], or Apiezon[3, 11] wax. Apiezon wax is the insulator of choice because unlike the nail polish, this material is a solid that can easily be melted onto the EC-etched probe. Additionally, Apiezon wax is relatively inert and etch resistant which is great for working in an electrolyte solution with a potential applied to the solution and the probe.[12]

3.3.2: COATING APPARATUS

Unlike the EC-etching process, the process of coating a super sharp tip is quite difficult. This requires a steady hand, decent eyesight, and patience. This is because one has to hold the EC-etched probe with a pair of tweezers and using the coating apparatus to coat the probe. Where the coating apparatus can be seen in Figure 3.11, which is just a solder iron that has controlled heat, by a Variac Transformer, onto a copper platform at the end of the solder iron. This platform has a small slit (roughly 1 mm in width) that is used to allow the probe to go inside of, when there is melted wax over top of the slit. If one is not careful and touches the copper wall (of the slit) with the probe apex, then that probe will be ruined because the apex is very fragile, and any small collision will bend and/or dull the tip. This tedious and difficult coating process needed to be changed and made easier to produce probes efficiently; this was done by collaborating with Dr. Li, Jon Hatton, and John Decker to produce a new Coating Apparatus.

Figure 3.11: Old coating apparatus, where there is a copper platform melts the Apiezon wax where the heat is controlled by a Variac transformer.

3.4: NEW EC-ETCHING AND CAOTING APPARATUS

The collaborative effort to produce a new apparatus had the goal of creating a platform that moves in all three dimensions (x-, y-, and z- directions). This seemed to be a difficult task as the design that was originally suggested was denied due to the difficulty of developing the extremely small moving parts and/or the complexity of all other moving parts. In either case, a new design was needed, and inspiration was derived from that of a traditional optical microscope. An optical microscope has a platform that allows for movement in the three dimensions, where the x- and y-directions (horizontal and forward/backward directions, respectively) are controlled by an attachment that sits on top of the platform that moves in the z-direction (vertical direction). So, it was hypothesized that if the x- and y-direction attachments could be purchased and placed on top of a Lab-jack then this would help solve this issue. Fortunately, the parts were cheap and easily

accessible, unfortunately, the Lab-jack did not move vertically in a level fashion. This apparatus version was utilized for the EC-etching part of the overall apparatus and can be seen on the left side of Figure 3.12.

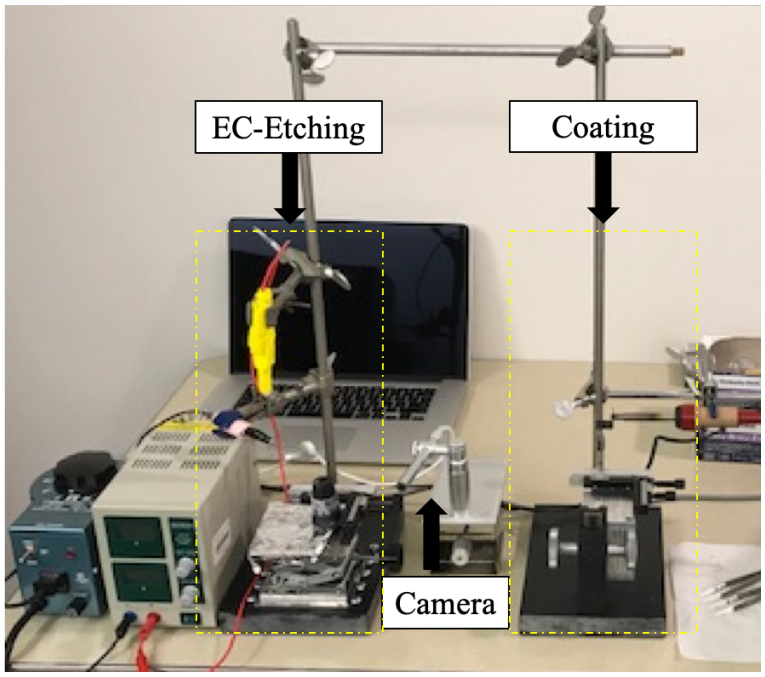

Figure 3.12: Image of the new EC-etching and coating apparatus where the left side is the EC-etching portion, the middle a microscope camera, and the right is the coating portion where the three-dimensional moving platform that hold a miniature chuck which hold the etched probe.

Luckily, there was a spare piece of an older microscope that was not in use, this piece allowed for the vertical movement and was used instead. Where a piece of aluminum was used to attach an aluminum platform to the older piece. The x- and y- direction attachments were screwed on top of this platform and a final piece of aluminum was screwed to the horizontal direction attachment. This aluminum piece has a hole drilled in it that allows for a miniature chuck to be placed and held. This chuck holds the EC-etched probe and is used to coat the probe. This apparatus was also combined with a microscope camera that connects to a computer so that the coating process can be more readily seen, see Figure 3.12.

This apparatus has shown to be quite helpful, as the process is no longer as difficult and has shown to be better than the previous method. In the method with the old apparatus a tip that was developed had the leaking current of over 100pA. Where the goal is to get 5pA or less of leaking current and multiple probes developed by this method has been accomplished. Additionally, the shape of the coating is better controlled with this apparatus. The shape plays a significant factor within probe development because there is a limited amount of space in the EC-cell and if the probe has too thick of a coating layer then this could push the RE and/or the CE which could cause a short circuit or the probe could collide with the cell cover which could damage the coating layer and/or build tension when the probe is approaching the sample, where, if the tension is built up enough it could damage the substrate when the tension is released.

Even though this new apparatus has come with great benefits to the development of the STM probes, controlling the shape of the EC-etched probe is still quite difficult. There are numerous types of shapes and the reasons for the shapes have continued to be elusive. However, the shape should not affect the results of the images that are developed as long as they have a sharp point at the apex of the probe, the apex is not bent, and if the probe is robust.

3.5: CHAPTER THREE REFERENCES

1. Ernst, S. Optimisation of the preparation process for tips used in scanning tunneling microscopy. Technische Universität Dresden, 2006.
2. Kazinczi, R.; Szocs, E.; Kalman, E.; Nagy, P., Novel methods for preparing EC STM tips. *Appl. Phys. A* **1998,** *66*.
3. Guell, A. G.; Diez-Perez, I.; Gorostiza, P.; Sanz, F., Preparation of Reliable Probes for Electrochemical Tunneling Spectroscopy. *Anal. Chem.* **2004,** *76* (17), 5218-5222.
4. Ren, B.; Picardi, G.; Pettinger, B., Preparation of gold tips suitable for tip-enhanced Raman spectroscopy and light emission by electrochemical etching. *Rev. Sci. Instrum.* **2004,** *75* (4), 837-841.
5. Khan, Y.; Al-Falih, H.; Zhang, Y.; Ng, T. K.; Ooi, B. S., Two-step controllable electrochemical etching of tungsten scanning probe microscopy tips. *Rev. Sci. Instrum.* **2012,** *83* (6).
6. Hagedorn, T.; El Ouali, M.; Paul, W.; Oliver, D.; Miyahara, Y.; Grutter, P., Refined tip preparation by electrochemical etching and ultrahigh vacuum treatment to obtain atomically sharp tips for scanning tunneling microscope and atomic force microscope. *Rev. Sci. Instrum.* **2011,** *82* (11).
7. Ekvall, I.; Wahlstrom, E.; Claesson, D.; Olin, H.; Olsson, E., Preparation and characterization of electrochemically etched W tips for STM. *Meas. Sci. Technol.* **1999,** *10*, 11-18.
8. Hobara, R.; Yoshimoto, S.; Hasegawa, S.; Sakamoto, K., Dynamic electrochemical-etching technique for tungsten tips suitable for multi-tip scanning tunneling microscopes. *e-J. Surf. Sci. Nanotech.* **2007,** *5* (0), 94-98.
9. Yau, S.; Fan, F.; Bard, A. J., In Situ STM Imaging of Silicon(111) in HF under Potential Control. *J. Electrochem. Soc.* **1992,** *139* (10).
10. Tuchband, M.; He, J.; Huang, S.; Lindsay, S., Insulated gold scanning tunneling microscopy probes for recognition tunneling in an aqueous environment. *Rev. Sci. Instrum.* **2012,** *83* (1).
11. Dijk, N. v.; Fletcher, S.; Madden, C. E.; Marken, F., Nanocomposite electrodes made of carbon nanofibers and black wax. Anodic stripping voltammetry of zinc and lead. *Analyst.* **2001,** *126* (11), 1878-1881.
12. Nagahara, L. A.; Thundat, T.; Lindsay, S. M., Nanolithography on semiconductor surfaces under an etching solution. *Appl. Phys. Lett.* **1990,** *57* (3), 270-272.

CHAPTER 4: ELECTROCHEMICAL CYCLIC VOLTAMMETRY STUDIES

4.1: EXPERIMENT

4.1.1: PURPOSE OF ELECTROCHEMICAL CV EXPERIMENTS

Electrochemical CV (EC-CV) is an extremely useful tool, especially when it is combined with EC-STM. Even though this study focuses on non-Faradaic processes, the adsorption/desorption of molecules to a substrate, which can help with exploring the influential parameters of the reaction. Such parameters include, potential dependency on the formation of two dimensional architectures that are the SNs on Au(111), concentration dependency of these structures, and electrolyte ion effect. It should be noted that the information from the CVs alone cannot conclude what structures are being formed and therefore should be used in combination with EC-STM to confirm the phase of the adlayer. However, CVs can provide potential regions that can be studied where different phases of the adlayer can be found, this is the potential dependency and has to be combined with EC-STM to observe the adlayer phase.

This chapter does not use CV in combination with EC-STM, instead, it focuses on the information collected from running multiple CVs to understand the concentration dependency with respect to how many potential regions can be explored with EC-STM. This is simply done by measuring CVs at respective concentrations of the molecule of interest, in this case varying the concentration of BZA. Additionally, to help understand the electrolyte ion effect and to help explain why there are no ordered SNs of 3 mM BZA in H_2SO_4 (see Chapter 5). The CV experiments of varied concentrations of BZA on Au(111) were either carried out in 0.1 M $HClO_4$, or performed in 0.05 M H_2SO_4. In order to be able to compare the CVs, the varied concentrations of BZA are the same throughout each experiment. Likewise, the pH of the solution remained around 1.00 for both experiments, which is why the concentrations of the electrolyte solutions are

0.05 M and 0.1 M for H_2SO_4 and $HClO_4$, respectfully; the amount of BZA affecting the pH of the solution is negligible for any concentration of BZA in either experiment.

4.1.2: RANDOM AND SYSTEMATIC ERROR

The random error with the CV measurements is seen as noise that produced based on the limits of the instrument and its ability to measure small values of current while controlling the applied potential or potential sweep at a set number of points measured per second, in addition to controlling the scan rate (the speed at which the potential changes, V/s). Alternatively, the systematic error, is the shifts of the peaks as a function of time. The location of the peaks with respect to the potential applied to the sample (x-axis of the CV) will change over time and has shown to go only in the positive directions (towards the right on the x-axis). This error is due to using a Pt wire as a quasi-RE instead of an actual RE. Traditional RE electrodes cannot be used in these experiments due to their size and inconvenience of cleaning. But the systematical error (shift of the reference potential) is quite small, about 0.005 – 0.020 mV shift during an entire CV experimental period, about 1 – 2 hours.

4.1.3: PROCEUDRE OF THE EC-CV EXPERIMENTS

4.1.3.1: CLEANING EQUIPMENT

All glassware was storied in a 2L beaker full of 18 M H_2SO_4 (Sigma Aldrich ACS reagent , 95-98%) for a minimum of 48 hours before use. This concentrated H_2SO_4 can oxidize the organic contaminates existing on the surface of glassware. This glassware includes, glass pipettes, 4-dram (15 mL) vials, and multiple beakers ranging from 10-150 Milliliters (mL) in volume. Additionally, Eppendorf 1000 Microliters (μL) pipette tips were stored in the same solution. The Teflon 125 mL bottles, O-rings, Cell Covers, and tweezer were all cleaned with Piranha solution.

Piranha solution is very dangerous and extreme caution should be used when working with the solution, it is an extremely strong oxidizer and very corrosive. Safety goggles, lab coat, and gloves should be worn at all times when working with this solution. Piranha solution is made of the volume ratio 3 parts 18 M H_2SO_4 (Sigma Aldrich ACS reagent, 95-98%) and 1 part 30% H_2O_2 (Alfa Aesar, 29-32%) (3:1). Where the H_2O_2 should always be added first to an empty container and the H_2SO_4 should be added second while completely filling the container to the desired volume. This is because the solution will be mixed as the H_2SO_4 is added to the solution, doing it the other way around will lead to an improper mixing of the two solutions and can cause an explosion. Once cleaned with Piranha or retrieved from the 18 M H_2SO_4 reservoir, the equipment was rinsed thoroughly with ultra-pure water known as Milli-Q water, which is from the purification system Direct-Q 3 UV Ultrapure (Type 1) water, that has a resistance of 20 MΩ or greater.

4.1.3.2: PREPARING SOLUTIONS

After the equipment has been cleaned either with 18 M H_2SO_4 or Piranha solution and rinsed thoroughly with Milli-Q water, the control and sample solutions were prepared. The control solutions were prepared by using either 18 M H_2SO_4 (99.999%, Sigma Aldrich) or 11.7 M $HClO_4$ (99.999%, Sigma Aldrich) to dilute them to either 0.05 M or 0.1 M, respectively, with the Milli-Q water. The sample solutions were prepared by first weighing out the desired mass of benzoic acid that is typically used as a standard for elemental analysis from Sigma Aldrich for the desired concentration. Afterwards, either the 18 M H_2SO_4 or the 11.7 M $HClO_4$ solutions used in the control solution, is used to make the same dilution as the control with Milli-Q water, such that both the control and the sample solutions have the same electrolyte and electrolyte concentration. Finally, the sample solution was either slightly heated and sonicated for an hour or heated until gently simmering for ten to fifteen minutes to dissolve the benzoic acid in solution.

The dilutions were done by either removing drops of the solution that sits in the cell-well and adding drop wise of either the concentrated sample solution or the control solution (which were previously made in the Teflon bottles) for the dilutions, or, by making the dilution in 15-dram vials prior to the cell assembly with a 1000 μL Eppendorf pipette. Both methods have their advantages and drawbacks, for example, the method with the Eppendorf pipettes help with making a more accurate measurement in volume to give the concentration of the solution more accuracy, however, it allows for more contamination because more equipment is being used. Whereas, the method that exchanges volumes of the solution in the cell-well by drops of solutions doesn't have as much accuracy, however, it is a quicker method which helps limit the time contamination has to collect on the surface of the Au crystal. The concentration of each solution can be seen in the Measurements and Solution Exchange section (section 4.1.3.4).

4.1.3.3: FLAME ANNEALING AND EC-CELL ASSEMBLY

The four trusted processes that are used to clean the equipment are Milli-Q water, Piranha solution, Argon (Ar) stream (for drying and/or cooling), and flame annealing with a butane torch. The equipment that is not cleaned with Piranha solution are the CE, RE, and WE. The Pt-CE and the Pt-RE are cleaned by flame annealing them until they are red/orange in color. The Au-WE is also flame annealed; however, it is flame-annealed in the dark for the safety of the Au crystal to distinguish the color (temperature) of crystal well. The stopping point for flame annealing the Au crystal is a slightly brighter red/orange color, however, it should not get to the point/color of a bright yellow. If this was done in a well-lit area, then by the time this color would be seen the Au crystal would be damaged as it had begun to melt. The goal is not to melt the Au crystal, instead to heat it to roughly 550-600°C that changes the color of the crystal to a bright red/orange for approximately 3 minutes, which is lower than its melting point[1]. The flame-annealing is for getting

rid of surface contamination or organic molecules from previous experiments, and for promoting a good the crystal lattice formation of 1,1,1 (111) surface. The way to cool the crystal while keeping away from adsorption of contaminates is by quenching it with Milli-Q water or by cooling with a rapid stream of Ar.

After the Au crystal has been quenched or cooled from the flame annealing, one has to be quick, the longer the Au crystal is exposed to the air the more contaminates can collect on the surface. At this point the cell assembly will also need to be done quickly and carefully, to ensure the cleanliness of the crystal. The Au crystal is place on the EC-STM cell plate, then the Teflon O-ring is retrieved from a sulfuric acid bath (and rinsed with Milli-Q water) or from a Milli-Q water bath and dried with either Ar stream or a heat gun before placing on top of the Au crystal. The same thing is done with the Teflon cell cover and it is placed on top of the Au crystal and O-ring which is all held in place by two metal clips holding all of the equipment down. Next, the control solution should be placed in the cell-well and at this point the Au crystal will be protected by the covering electrolyte solution and is less likely to collect contamination with a solution covering the Au surface.

At this point the control solution is in the cell-well, however, one needs to check for leaks because it would be disappointing to let an experiment go to waste if all of the solution leaks out and CV measurements can't be made or by letting contaminates get to the surface before refilling the cell-well with the control solution. Once it has been confirmed there is no leaks with the cell, then the Pt counter and reference electrodes can be connected to the cell and submerged into the solution. Next, one should check the connections of each point of the circuit in the cell plate and the electrodes with a multimeter. If the connections are good then the cell has been successfully

assembled, see Figure 4.1. The assembled cell can be integrated with the instrument and measurements can take place.

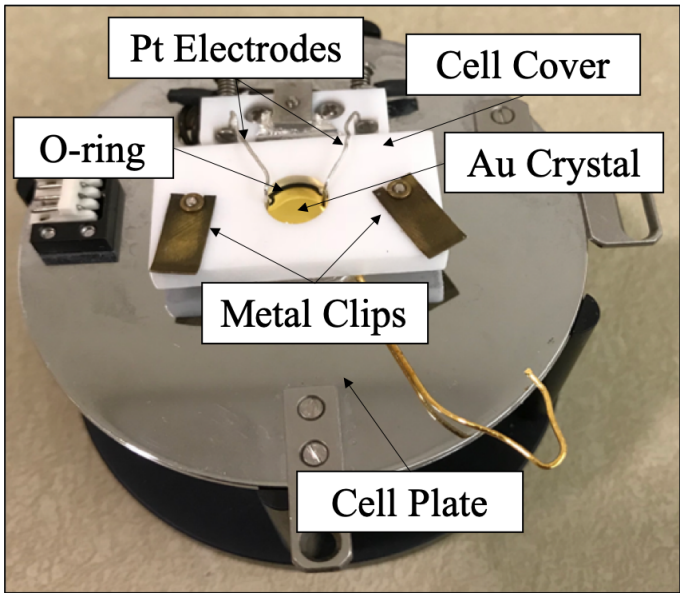

Figure 4.1: Assembled EC-cell with a Au substrate that is a model for how each experiment should be set up whether the experiment only calls for EC-CV, EC-STM imaging, or both.

4.1.3.4: MEASUREMENTS AND SOLUTION EXCHANGE

Once the assembled cell with the control solution is integrated into the instrument, 10 cycles of a continuous CV are measured to get rid of reconstruction lines. Reconstruction lines are seen a z-direction buckle of atoms where there are bright lines in a crystal lattice. Running a CV in multiple cycles helps to get rid of the reconstruction lines, which is a phenomenon of reconstruction of surface gold atoms due to the thermal annealing. The removal of reconstruction lines can be seen in the multi-cycled CV where the space in between each cycle gets closer to zero amperes, see Figure 4.2.

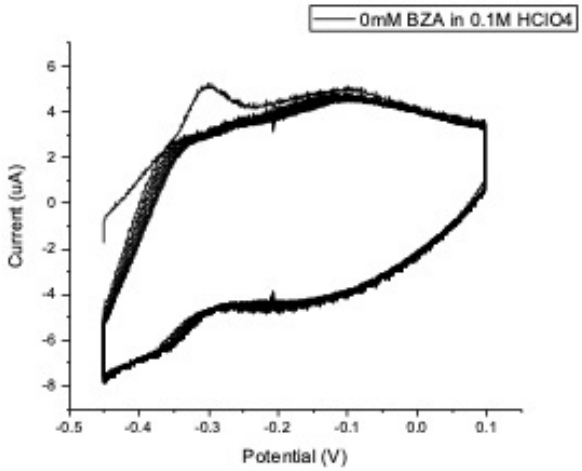

Figure 4.2: CV of only 0.1 M $HClO_4$ on Au(111) with 10 complete cycles which show the removal of reconstruction.

At this point, one can either run a CV of the control solution in a way that the rest of the concentrations would be measured and then exchange the solution. The solution exchange should be done with extreme diligence because at this is a point many things can go wrong. For example, if one is trying to keep control of the potential, do not remove so much solution from the cell-well that the counter or the reference electrodes are no longer submerged in the solution. To control the potential when adding a solution, let the drop fall on the reference electrode and into the cell-well rather than placing the solution directly into the solution. Additionally, be mindful where the pipette tip is relative to the Au crystal, it is possible to crash the glass pipette into the Au crystal when withdrawing the solution, which would damage the Au crystal and potential add contaminates, such as pieces of broken glass in the solution and on the Au crystal surface. Finally, making sure to perform the exchange five to six times, mixing in between each exchange, is done to ensure the previous solution has no effect on the measurement that would follow previous measurement.

4.2: CYCLIC VOLTAMMOGRAMS OF Au(111) IN H_2SO_4 AND IN $HClO_4$

After imaging 3 mM BZA in 0.05M H_2SO_4 it was thought that there might be an electrolyte ion effect which might be competing with the BZA to adsorb to the surface. This is what lead to a switch of the electrolyte solution to 0.1 M $HClO_4$. Yet, after getting similar results with the new electrolyte solution, it was thought that the concentration of BZA could be playing a larger role than the electrolyte ion effect. This is the purpose of comparing both electrolyte solutions with the varying BZA concentrations.

The CVs show similar characteristics of an EC-reversible reaction for Faradaic processes; however, the reaction of the molecules adsorbing is reversible, they can desorb from the substrate. Yet, this reaction is not the same as an EC-reversible reaction for Faradaic processes because there is no charge transfer reaction taking place. Additionally, the Pt-RE is not an ideal type of reference electrode because the peaks measured in a CV can change its position with respect to the potential (x-axis) over time. However, it can be seen, like in an EC-reversible reaction for Faradaic processes, that as the scan rate of the potential sweep increases so does the magnitude of each peak in the CV, which can be seen in Figure 4.3.

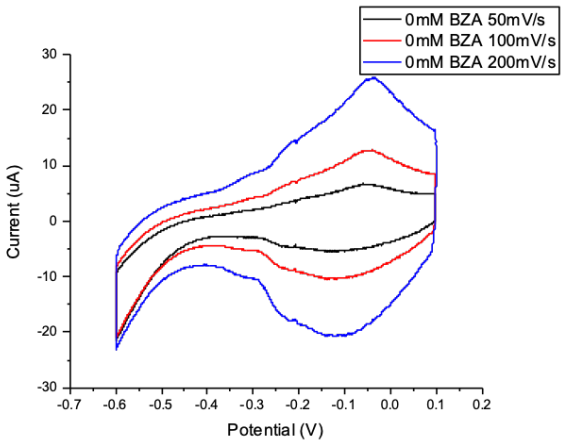

Figure 4.3: The CVs overlapped on one plot, where each measurement was done with the same solution of 0 mM BZA in 0.05 M H_2SO_4 but with different scan rates, which were 50, 100, and 200 mV/s.

The CVs of just the electrolyte solutions has a distinct difference which supports the thought of an electrolyte ion effect, which is that the 0.05 M H_2SO_4 CV shows a small broad peak at roughly -0.05V, a sharp intense SO_4^{2-} adsorption peak at higher positive potentials can be seen in literature for this control solution.[2] This is due to the adsorption of SO_4^{2-} anions on Au(111) surface in the control solution. Whereas, 0.1 M $HClO_4$ CV shows less of broad peak in the same potential window of Figure 4.3. These features can be seen in Figure 4.4.

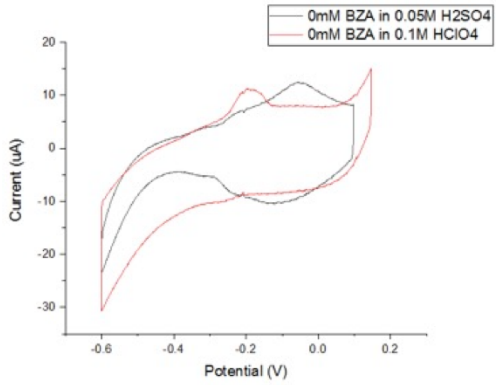

Figure 4.4: CV of both 0 mM BZA in 0.1 M $HClO_4$ and 0 mM BZA in 0.05 M H_2SO_4 control at the scan rate of 100 mV/s.

4.3: CVs OF Au(111) IN H_2SO_4 WHILR IN THE PRESENCE OF BENZOIC ACIDS

In this experiment, it has been concluded that there are no more than one large broad peak in all of CVs measured for BZA at the concentrations of 0, 2, 3, 4, 6, 8, 10, 12, 14, 16, 18, 20, and 23 mM in 0.05 M H_2SO_4. These CVs can be seen in Figure 4.5, where no transition point between the one broad peak to multiple peaks are observed.

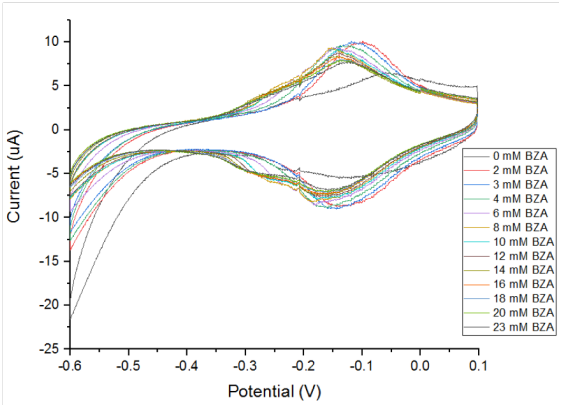

Figure 4.5: This overlaid CV shows all of the varied concentration of BZA (0-24 mM) in 0.05 M H_2SO_4 where it can be seen that only one peak is found at each concentration and that there are no other potential regions to be explored.

It is possible that the procedure of experiment was not at the same level that it needed to be, and sources of contamination could have prevented good observations. Or, perhaps there is a very strong electrolyte ion effect, and this alone prevents the transition between one broad peak to multiple sharp peaks, like that with the $HClO_4$ electrolyte (see Chapter and Section 4.4). To be certain, this experiment needs to be repeated to verify that these results are reproducible or not, even under the best conditions for the experiment.

Currently, there has not been enough time to run this experiment. When this experiment can be run, it would be beneficial to measure CVs of BZA at 0, 0.6, 1, 3, 4, 6, 8, 12, and 24 mM BZA in 0.05 M H_2SO_4. This results in less measurements which makes the experiment easier and more comparable to the CVs measured at the same concentrations of BZA in 0.1 M $HClO_4$ (see Chapter/Section 4.4). However, if no transition between one broad peak to multiple sharp peaks are seen at the concentrations of 12 mM BZA or lower, then perhaps there should be more measurements between the concentrations of 12 mM to 24 mM BZA in 0.05 M H_2SO_4.

4.4: CVs OF Au(111) IN $HClO_4$ WHILE IN THE PRESENCE OF BENZOIC ACIDS

It is readily seen that the CV of Au(111) in perchloric acid electrolyte at a higher concentration of BZA results in three peaks which give four potential regions to explore. This CV measurement is of 20mM BZA in 0.1M $HClO_4$ see Figure 4.6.

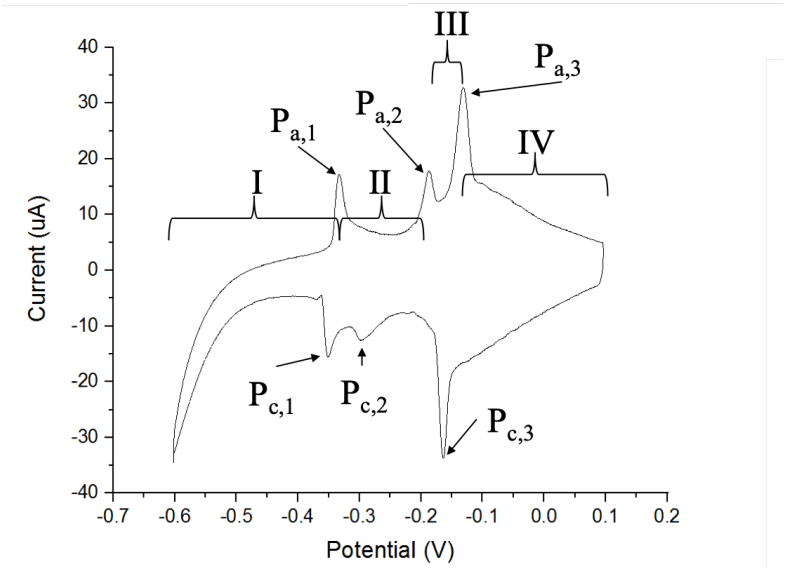

Figure 4.6: CV of 20 mM BZA in 0.1M $HClO_4$ that contained three potential regions that can be explored with EC-STM imaging. The anodic peaks are labelled from left to right as $P_{a,1}$, $P_{a,2}$, and $P_{a,3}$ and the cathodic peaks) are labelled from left to right as $P_{c,1}$, $P_{c,2}$, and $P_{c,3}$.

This CV was an attempt to see more adsorption peaks at a reasonably high concentration after the CV of 3 mM BZA in 0.1 M $HClO_4$ was measured and imaged where only disordered phases were found on either side of the peak (see Chapter 5). At the 3 mM BZA concentration only one broad peak is seen, and it is very similar to the CV of 3 mM BZA in 0.05 M H_2SO_4 (see Figure 4.7).

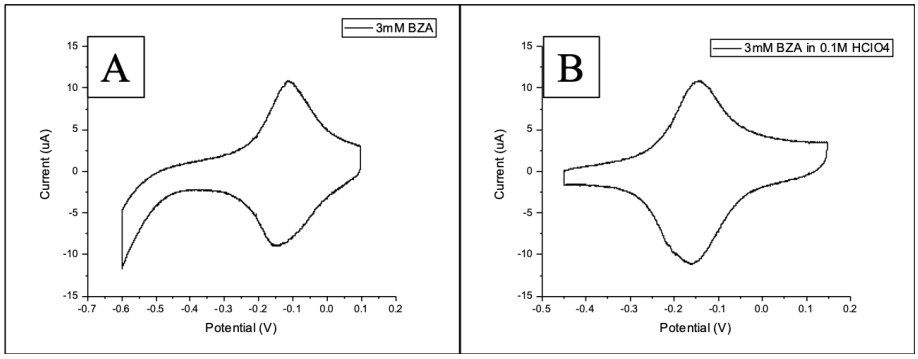

Figure 4.7: CVs of 3 mM BZA in 0.05 M H_2SO_4 (A) and 3 mM BZA in 0.1 M $HClO_4$ (B).

After finding no ordered long ranged SNs, it was thought that the concentration of the BZA needed to be increased.

BZA, at roughly 300 K, is reported to be soluble in water (in non-electrolyte) up to the concentration of roughly 30 mM.[3] Solutions close to this concentration, at 24 mM BZA in 0.1 M $HClO_4$ has shown to develop a visible thin film precipitate. Perhaps this is because the pH of water (7) is higher than BZA's pKa (~4.2) which leads to a majority of deprotonated BZA (benzoate) molecules which is more soluble in water. Opposed to the pH of the electrolyte solutions (1) which leads to a majority of protonated BZA molecules which would be less soluble. However, another complication was found in previous experiments, which was a lack of cleanliness in the solution and/or equipment. This error was most likely done in either the cleaning of the equipment and/or the solution preparations. The contamination is understood to compete with the BZA to adsorb onto the surface of the substrate which distorts the CV as the merging of A/D peaks happens at higher concentrations, this can be seen in Figure 4.8.

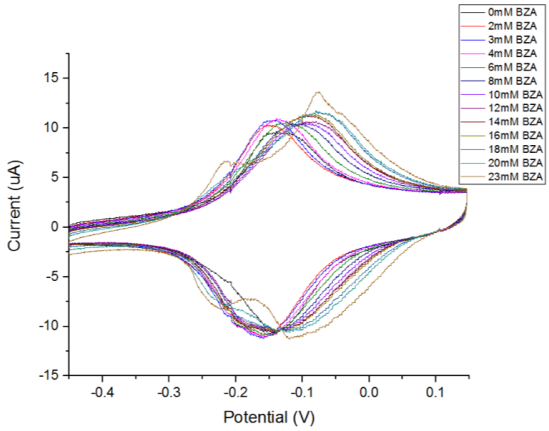

Figure 4.8: CVs of varied concentration of BZA (0-23 mM) in 0.1 M $HClO_4$ where it can be seen that peaks change at a certain concentration of BZA, allowing for more potential regions to be explored.

This mistake was then rectified by altering the sample preparation protocol by using the "double beaker" method for the dilution of the acid for the electrolyte solution. From this past experiment it should be known that the bottle that holds the very pure acid is not clean. Thus, there should be two cleaned beakers (with Piranha solution, Milli-Q water, and dried) inside one another (a 50 mL and a 10 mL beaker) where the goal is to fill the 10 mL beaker with the concentrated acid by letting it flow into the large beaker first. Then with a continuous stream move the flow of the acid into the 10 mL beaker until full. This method was used for the following trail of the CV experiment for the following solutions: 0, 0.6, 1, 3, 4, 6, 8, 12, and 24 mM BZA in 0.1 M $HClO_4$. Where solutions of 0 to 4 mM BZA in 0.1 M $HClO_4$, at best, had one broad peak, this can be seen in Figure 4.9.

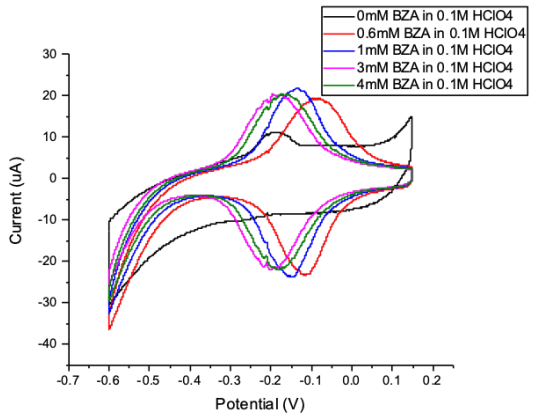

Figure 4.9: CVs of the varied concentrations (0-4 mM) of BZA in 0.1 M $HClO_4$.

However, at concentrations at 6 mM BZA or greater in 0.1 M $HClO_4$ there are multiple sharp peaks observed, see Figure 4.10.

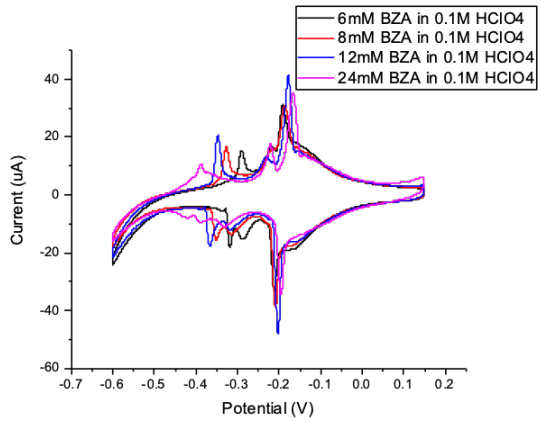

Figure 4.10: CVs of the varied concentrations (6-24 mM) of BZA in 0.1M $HClO_4$.

Where, roughly around 6mM BZA in 0.1 M $HClO_4$ is the transition point, which allows for more adsorption phases to be observed. However, after further examination of the CVs of 6, 8, 12, and 24 mM BZA in 0.1 M $HClO_4$ it is seen that the peaks become more clearly defined the higher the concentration of BZA, refer to Figure 4.11.

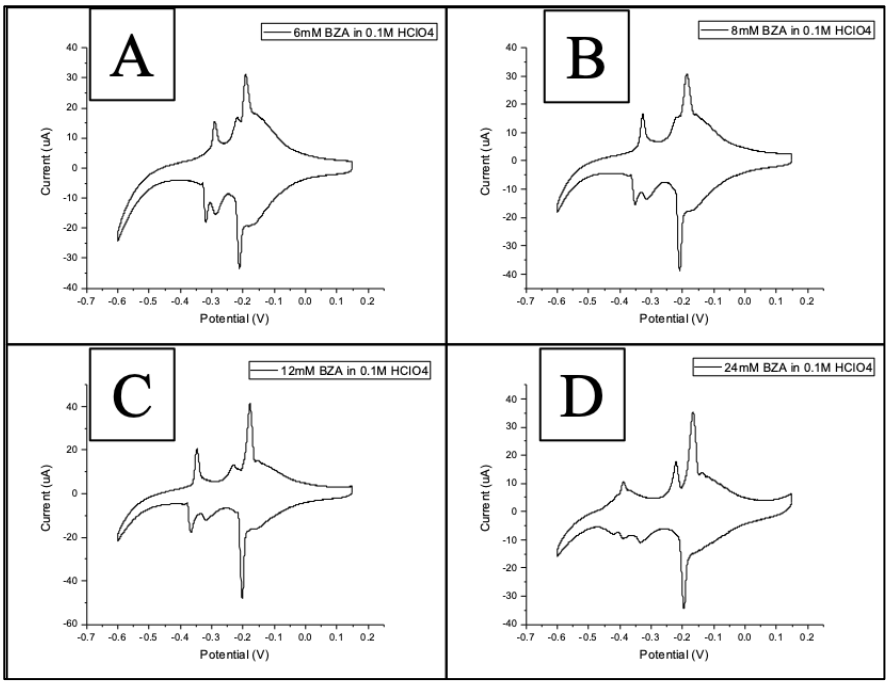

Figure 4.11: Individual CVs of the varied concentrations (6-24 mM) of BZA in 0.1 M $HClO_4$ where (A) is at 6 mM BZA, (B) is at 8 mM BZA, (C) is at 12 mM BZA, and (D) is at 24 mM BZA 0.1 M $HClO_4$

Additionally, the peak separation increases between peaks $P_{a,1}$ and $P_{a,3}$ as BZA concentration increases. Figure 4.12 helps to visualize these features; it also shows where the peak potential is located at the various concentration of BZA.

Where each plot in Figure 4.12 appears to be linear, as a result the following data is the y-intercept (b) and slope (m) with their respective r-squared (r^2) values. Figure 4.12A $P_{a,1}$ b is -0.179 V, m is -0.066 V, and r^2 is 0.946; $P_{a,2}$ b is -0.203 V, m is -0.0067 V, and r^2 is -0.220; $P_{a,3}$ b is -0.225 V, m is 0.0184 V, and r^2 is 0.994. Figure 4.12B $P_{c,1}$ b is -0.272 V, m is -0.037 V, and r^2 is 0.994; $P_{c,2}$ b is -0.241 V, m is -0.030 V, and r^2 is 0.984. Figure 4.12C b is -0.0452 V, m is 0.085 V, and r^2 is 0.969.

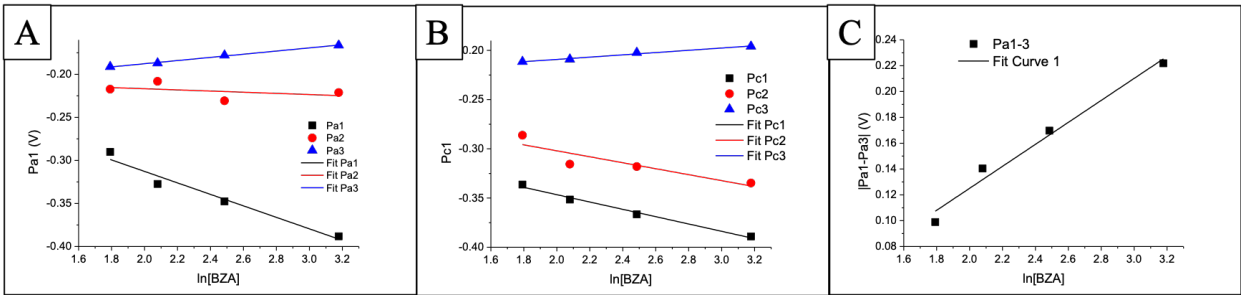

Figure 4.12: (A) is a plot of the location as potential vs. [BZA] for peaks $P_{a,1}$, $P_{a,2}$, and $P_{a,3}$. (B) is a plot of the location as potential vs. [BZA] for peaks $P_{c,1}$, $P_{c,2}$, and $P_{c,3}$. (C) is a plot of the absolute value of the change in peak potential between $P_{a,1}$ and $P_{a,3}$ vs. [BZA].

For EC-STM imaging purposes, it is best to be at a concentration of BZA higher than 6 mM but lower than 24 mM BZA in 0.1 M $HClO_4$ to both obtain a good quality CV to make better observations at potential in between the adsorption peaks and to prevent the recrystallization BZA in the solution. The reason why the peak separation change as a function of BZA concentration will be discussed in Chapter 5 after the molecular structures and adlayers are imaged.

4.5: CHAPTER FOUR REFERENCES

1. Sambles, J. R., An Electron Microscope Study of Evaporating Gold Particles: The Kelvin Equation for Liquid Gold and the Lowering of the Melting Point of Solid Gold Particles. *Proc. R. Soc. Lond. A.* **1971,** *324*, 339-351.
2. Li, Z.; Wan, L. J.; Wandlowski, T., Supramolecular Nanostructures of 1,3,5-Benzene-tricarboxylic Acid at Electrified Au(111)/0.05M H_2SO_4 Interfaces: An in Situ Scanning Tunneling Microscopy Study. *Langmuir* **2005,** *21* (15), 6915-6928.
3. Apelblat, A.; Manzurola, E.; Abo Balal, N., The solubilities of benzene polycarboxylic acids in water. *J. Chem. Thermodynamics* **2006,** *38* (5), 565-571.

CHAPTER 5: SCANNING TUNNELING MICROSCOPY STUDIES

5.1: EXPERIMENT

STM is used to develop images of conductive surfaces and interfaces in order to understand atomic arrangement of a solid, adsorption properties, or the self-assembly of compounds adsorbing on a surface in this project.[1-3] Where the general procedure for cleaning the equipment and solution preparation is the same as previously stated in Chapter 4. Prior to cleaning the equipment an STM probe should have already been made and placed into the instrument, see Chapter 3. Where a difference between imaging experiments and CV experiments is that depending on the type of STM environment, a CV measurement cannot be collected (ambient or UHV STM). However, if the system is running under EC-STM then the probe is submerged into the electrolyte solution and is only but a few nanometers away from the surface of the substrate. The introduction of a second, WE, which is the STM probe, will not affect the CV measurement in any noticeable way.

Yet, CV measurements can still be collected while scanning/imaging is taking place which is often done throughout EC-STM studies. An additional difference between the two procedures is that after the reconstruction lines have been removed by running a few complete cycles of the CV potential sweep with the control solution. The control solution must then be exchanged with the sample solution properly before integrating the EC-cell with the instrument so that imaging measurements can be made. The process of removing the reconstruction lines with CV is not seen under ambient or UHV conditions because a CV measurement can only be collected under EC-STM.

5.2: AMBIENT STM: HIGHLY ORIENTATED PYROLYTIC GRAPHITE (HOPG)

EC-STM was not the first measurement made throughout this project, which because when training an individual with STM, it is often a useful method of teaching to use an easier technique

and then move up to a more difficult one. In this case, Ambient STM is much easier than EC-STM because it does not require such intense efforts of cleaning, assembling an EC-cell, nor is there a requirement of the tip being coated with an insulting material. Thus, training with ambient STM was done by attempting to image HOPG with a Pt/Ir probe. Where the Pt/Ir probe was mechanically fabricated by cutting a Pt/Ir (70%:30%) wire with a special STM tip cutter, so called a mechanical sharpening technique.

The process of preparing this substrate in comparison with the Au crystal, is much easier. Flame annealing this substrate is not necessary because cleaning this HOPG substrate is similar to cleaning mica (see Appendix), where cleaving layer by layer can be done by using a scotch tape. Additionally, HOPG begins to have a rough surface when exposed to temperatures around 493 K[4], so flame annealing with a butane torch can be problematic. Similar with techniques found in Chapter 2, the probe needed to sit in the instrument for 24-48 hours to reduce the amount of z-drift and increase the stability of the instrument before a reasonable measurement was produced. Figure 5.1 shows one of the images developed from this technique, where the brighter spots represent carbon atoms (outlined in blue) and the dark areas represent the space between carbon atoms (outlined in green).

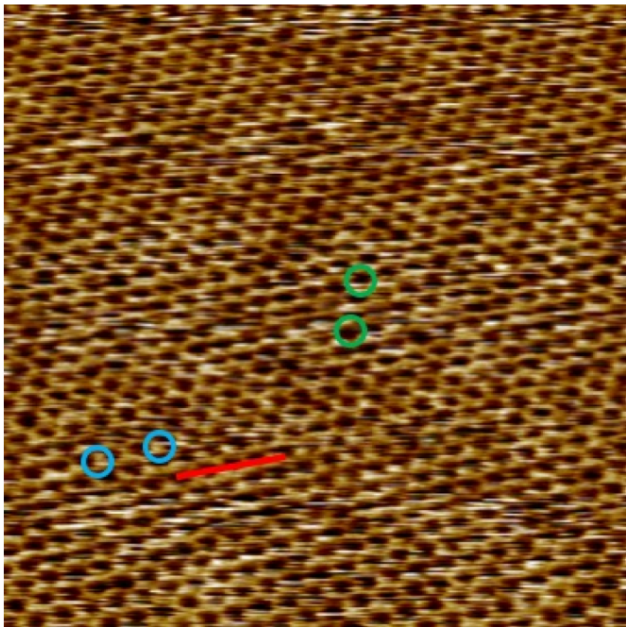

Figure 5.1: 5x5 nm in-air STM image of HOPG with Pt/Ir probe where the bright spots are representative of carbon atoms (outlined in blue) and the dark areas are representative of the spaces between carbon atoms (outlined in green).

The following cross section was then measured from the image itself to measure a rough estimate of how far the atoms are from one another, in figure 5.2. The distance between two adjacent carbon atoms is roughly 0.24 nm, which is consistent with the size of a carbon atom and the literature.[5]

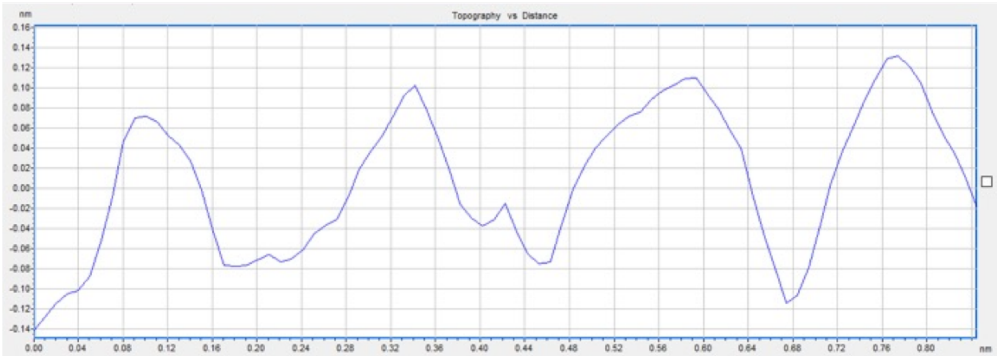

Figure 5.2: The cross section of Figure 5.1 where the x-axis on this plot is seen as the red line in Figure 5.1. This cross section allows the relative height of each carbon atom with respect to the lowest value measured in the STM image.

5.3: EC-STM STUDY OF BENZOIC ACIDS (BZAs) ON Au(111)

The following sub-sections are in chronological order with how the experiments took place to better communicate the evolution of the study and the thought process behind performing the following studies. Where BZA was an interesting molecule to study as a building block for SNs because of it only having one CAFG in comparison to IA and TMA. The work with TMA under EC-STM was the ideal work to compare this project to which is why 3 mM BZA in 0.05 M H_2SO_4 was chosen. TMA was used to study 3 mM TMA in 0.05 M H_2SO_4 on Au(111). At this concentration of TMA there were five different SNs observed.[6]

5.3.1: 3 mM BZA IN 0.05 M H_2SO_4

The measured CV with 3 mM BZA in 0.05 M in H_2SO_4 is already apparently different from the CV with TMA, see Figure 4.7. That is, this CV has only one broad peak with two potential regions to explore, to the left and the right of the peak. At a potential left of the adsorption peak, there was a disorder phase. This disorder phase can be seen in Figure 5.3A and 5.3C, as there may be some substrate features below the adlayer but without any ordered molecular adlayer/pattern features on top of the surface, this adsorption phase is defined as disordered.

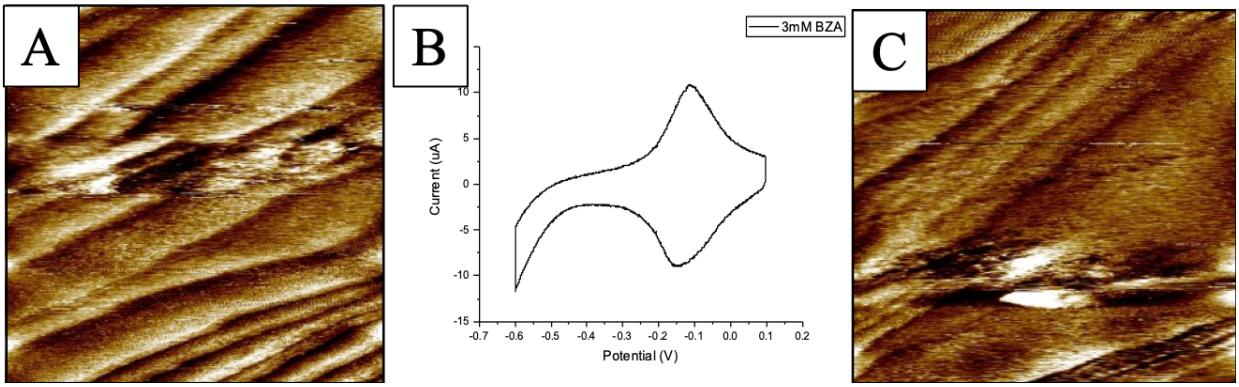

Figure 5.3: (A) EC-STM image of 3 mM BZA in 0.05 M H_2SO_4 at E_S = -0.350 V which is left of the adsorption peak found in the CV. (B) is the CV of 3 mM BZA in 0.05 M H_2SO_4. (C) EC-STM image of 3 mM BZA in 0.05 M H_2SO_4 at E_S = 0.200 V which is right of the adsorption peak found in the CV.

A similar disordered phase is seen at a potential right of the adsorption peak, in Figure 5.3B and 5.3C. After an attempt to repeat this experiment resulted in a similar outcome, it was hypothesized that perhaps there is something such as sulfate ions competing with BZA adsorption on the substrate.

Contamination can also compete with the BZA, however, after a meticulous procedure put forth into this experiment, it was thought that, in this case, that this was not the main competitor. Instead, H_2SO_4 might be the larger influence on the results, where H_2SO_4 is a strong acid and will dissociate to sulfate anion, SO_4^{2-}. Knowing that the sulfur on thiols bind really well to an Au surface[7], that perhaps there is a strong competing factor of SO_4^{2-} adsorbing to the substrate, or, maybe there is simply an ion effect with the electrolyte. This led to the change of the electrolyte solution to 0.1 M $HClO_4$. At this concentration of perchloric acid, the pH of the solution is the same as the sulfuric acid electrolyte, which is roughly 1, and the Hydronium Ion (H_3O^+ or H^+) concentration should be roughly 0.1 M.

5.3.2: 3 mM BZA IN 0.1 M $HClO_4$

Similar to 3 mM BZA in 0.05 M H_2SO_4, 3 mM BZA in 0.1 M $HClO_4$ results in a similar CV, which is seen in Figure 5.4.

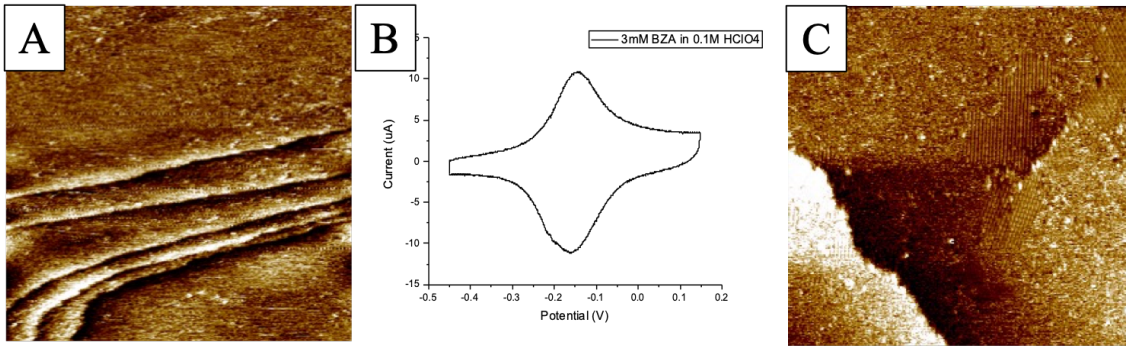

Figure 5.4: (A) EC-STM image of 3 mM BZA in 0.1 M $HClO_4$ at E_S = -0.200 V which is left of the adsorption peak found in the CV. (B) is the CV of 3 mM BZA in 0.05 M $HClO_4$. (C) EC-STM image of 3 mM BZA in 0.1 M $HClO_4$ at E_S = 0.500 V which is right of the adsorption peak found in the CV.

Where to the left of the adsorption peak there is a disorder phase, which can be seen in figure 5.4A and 5.4B. Likewise, in Figure 5.4B and 5.4C, to the right of the adsorption peak there is another disorder phase but with some small patches of locally ordered areas decorated. Due to the similarities of this study with respect to the previous study with the 0.05 M H_2SO_4 electrolyte solution, it was hypothesized that perhaps the number of peaks that can be measured with CV is more dependent on the concentration of the adsorbing species. If there are more peaks that appear in a CV for non-Faradaic processes, then it is thought that there are more transition points between adsorption phases. Where the potential ranges between peaks are the regions to best observe individual adsorption phases (refer to Chapter 2). So, the concentration of BZA was raised to 20 mM in 0.1 M $HClO_4$, low enough so that nothing would recrystallize and high enough to see if concentration does play a role in the formation of two dimensional SNs.

5.3.3: 20 mM BZA IN 0.1 M $HClO_4$

The measured CV for 20 mM BZA in 0.1 M $HClO_4$ has a surprisingly interesting number of peaks and number of potential regions between peaks in Figure 4.6 (Chapter 4). Unfortunately, the images that were collected following the CV measurement did not appear to give any ordered

SNs or the images developed had too much artificial noise which resulted in not being able to make reasonable observations at the various potential regions in the CV during that experiment. Additionally, what features might be seen are not sharp which leads to the thought of the STM probe being dull, potential too dull to obtain a high-quality image at atomic resolution.

In any case, this experiment was halted as it was thought that no observation of the adsorption phases could be made. After this experiment, there was more of an interest geared toward making the observations that could not be collected from this experiment. At the same time, the problem of not knowing at what point does the transition between one to three peaks occur was still present. This is because this experiment and the following 12 mM BZA in 0.1 M $HClO_4$ experiment took place before the CV experiment of varied concentration of BZA in 0.1 M $HClO_4$.

5.3.4: 12 mM BZA IN 0.1 M $HClO_4$

The experiment where 12 mM BZA in 0.1 M $HClO_4$ had been the best experiment throughout this project. However, the data is not as beautiful as other published works of aromatic molecular adsorption nor were there enough observations to clearly distinguish the types of ordered adsorption phases. This is attributed to the fact that EC-STM requires experience, skills, patience, meticulous experimental habits, and time. Time to make mistakes and learn from those mistakes, however, to truly become an expert in EC-STM takes time. In any case, for this project, help was needed from Dr. Li when it was evident that high quality EC-STM images are difficult to be developed from this individual's attempts during a short and limited period of time.

Where, in these attempts, the following were the seemingly repeatable issues: STM probe coating allowed for too much leaking current to image, STM probe was not very sharp, too much contamination, and/or solution leaked or evaporated from the cell-well. With these, apparent issues

in previous attempts in this experiment, there was still an attempt that led to decent results/observations. This was where a linear pattern was observed, see Figure 5.5.

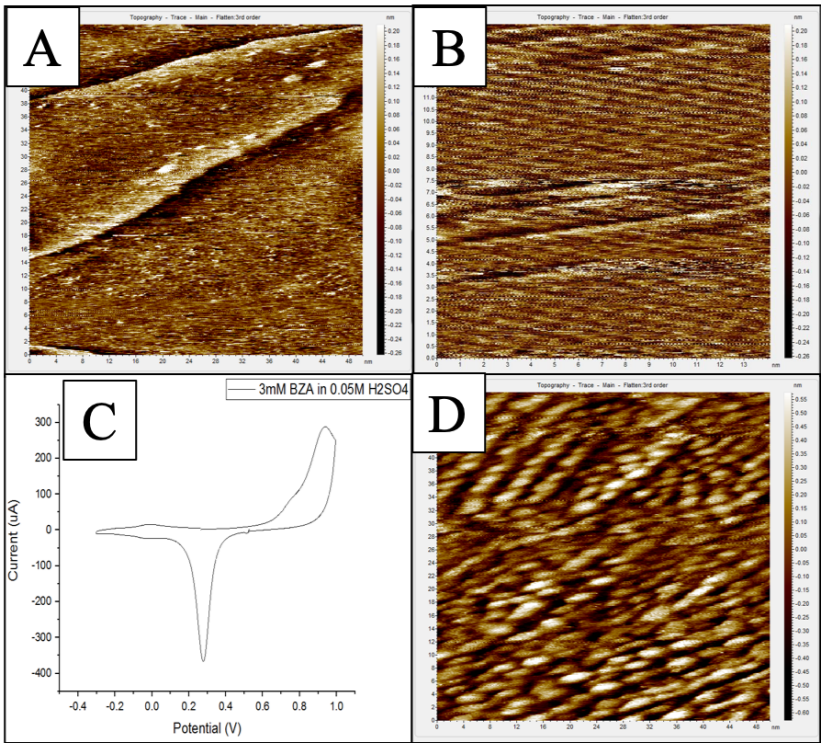

Figure 5.5: (A) is a disordered phase EC-STM 50 nm x 50 nm image at E_S = -0.200 V, (B) is a ordered phase EC-STM 14 nm x 14 nm image at E_S = -0.190 V, (C) is a CV at a large window that allows for oxidation and reduction of the Au crystal where peak on the right is the oxidation peak and the peak on the left is the reduction peak, (D) is an image of the Au crystal once it was oxidized where it can be seen that there is an rough surface due to this reaction, which was at E_S = 0.740 V.

. It can be seen in Figure 5.5, that the linear pattern allows for the hypothesis that there might be a dimerization between the CAFGs between adjacent BZA molecules, see Figure 5.6.

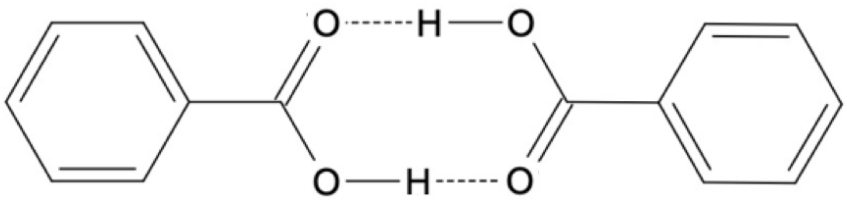

Figure 5.6: MolecularSketch drawing of the possible intermolecular hydrogen bonding interaction between two BZA molecules that is hypothesized from Figure 5.5.

This type of dimerization relates very closely to how the crystal structure of solid BZA is formed, see Figure 5.6.[8-9] However, the dimerization of BZA molecules cannot be verified without better atomic resolution. Some of the remaining imaging (Fig. 5.8, 5.9, 5.11) data that is presented in this chapter are compliments of Dr. Li.

The strategy to image the different potential regions of the CV measured at 12 mM BZA in 0.1 M $HClO_4$ was to perform a cathodic potential sweep (in the negative potential direction) until the potential region of interest is selected. When performing a cathodic scan, it allows for the molecules to have a better chance to form an adsorption adlayer due to the repulsive nature of the contaminates have with the negatively induced potential. Alternatively, when examining the anodic scan of each of the four regions, a cathodic scan was used in the CV and when the potential sweep approached the lower potential limit it switched directions and began sweeping anodically. This technique was used rather than starting from the lower potential limit and scanning.

Region I was seen and understood as a disorder adsorption phase due to the lack of long ranged patterns, which is seen in Figure 5.7B at the top third of the image.

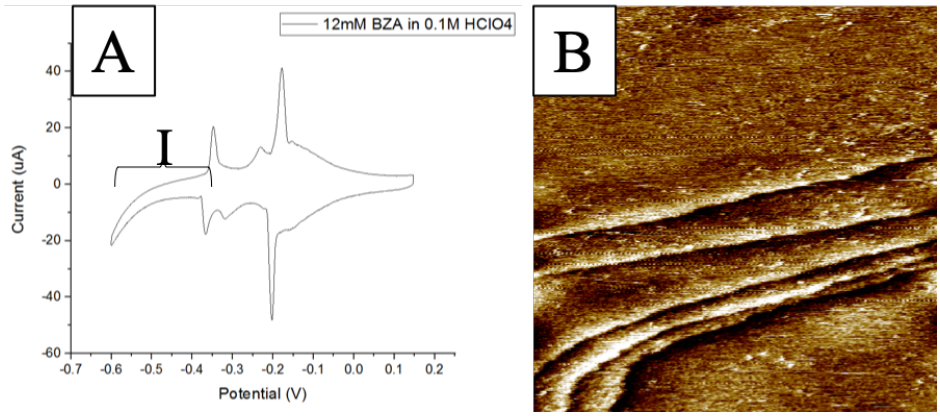

Figure 5.7: (A) is a CV measured of 12 mM BZA in 0.1 M $HClO_4$ from 0.150 V to -0.600 V that serves as a visual representation of the potential range that image (B) was collect. (B) is a disordered phase EC-STM image of 12 mM BZA in 0.1 M $HClO_4$ in region I.

Where the corresponding CV for the image is seen as well in the same figure. Where in this Figure, before the green arrow in the EC-STM image is found in the potential region I, after the green arrow is at the potential region of II. After the transition from region I to region II, an interesting observation was made.

Where in potential region II (between peak $P_{a,1}$ and $P_{a,2}$, see CV in Figure 4.6) there seems to be linear stripe patterns where there are significant spacings between each stripe, see Figure 5.8. It is seen in Figure 5.8 that the patterns of adsorbed molecules are at different heights relative to one another, which suggests that there are possibly multiple layers of adsorbed molecules or co-adsorbed ions.

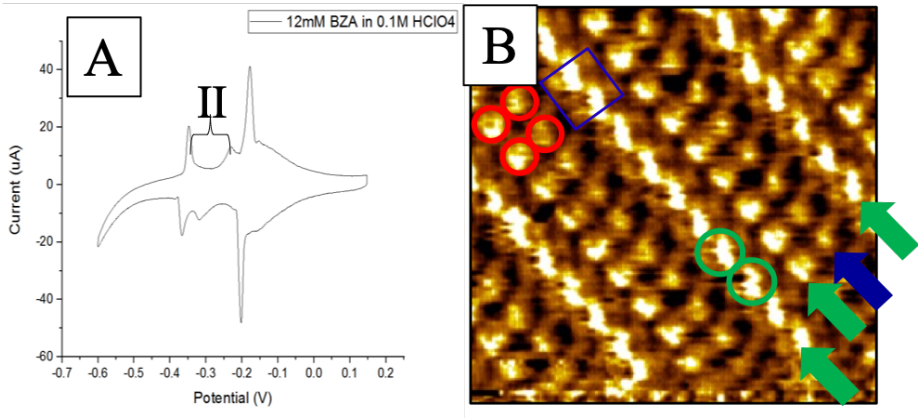

Figure 5.8: (A) is a CV measured of 12 mM BZA in 0.1 M $HClO_4$ from 0.150 V to -0.600 V, (B) is an EC-STM image where there seems to be BZA molecules in between each bright linear stripe. That is the bright linear stripes are made up of bright spots outlined in the green circles and green arrows, additionally, there a less bright spots in between the stripes that are outlined in the red circles and blue arrow.

This in turn is complex, where it is thought that perhaps there is a linear dimerization, indicated by the red circles. Additionally, the pattern outline by the green circles appear higher than the BZA dimers. Perhaps this species is on top of BZA molecules, this is only a speculation and cannot be determined with only STM techniques. The species that appears on top of the BZA molecules cannot be determined at this point either, perhaps it is the electrolyte ClO_4^-, at this point it is unsure. However, the BZA dimer is speculated to be similar to the H-bonding from CAFGs between adjacent BZA molecules, like that seen in Wilson et al. published work with benzoic acid dimers.[10]

Yet, in region III, there seems to be a pattern mixture where in Figure 5.9 an outlined zigzag pattern can be seen.

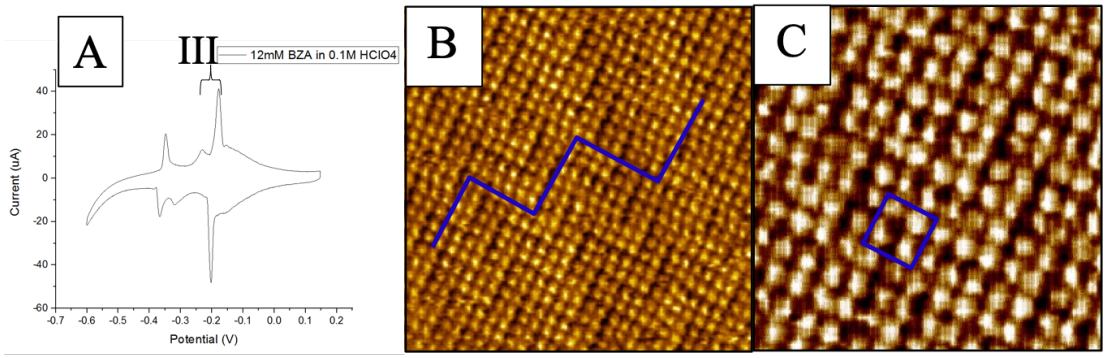

Figure 5.9: (A) CV measured of 12 mM BZA in 0.1 M $HClO_4$ from 0.150 V to -0.600 V, (B) and (C) are EC-STM images at region III at E_S = -0.075 V where (B) is 20 nm x 20 nm and (C) is 10 nm x 10 nm. It can be seen that there is a zigzag pattern in (A) that is outlined with a blue line. However, when zoomed in to (B) four BZA pointed towards the center of the square shape that is outlined by the blue square.

However, if one looks closely, the molecules are arranged in groups of four or as groups of two where there are a pair of groups to form a square pattern. These square shaped building blocks have a type of morphological feature where they are shaped similar to the thought BZA would be, where the CAFG is pointing towards the other three adjacent BZA CAFGs or towards the other adjacent BZA CAFG, for the group of four and the group of two, respectively. This is what led to the tentative proposed structural model where the intermolecular interaction of H-bonding seems highly dictates the formation of this zig-zag pattern and can be seen in Figure 5.10.

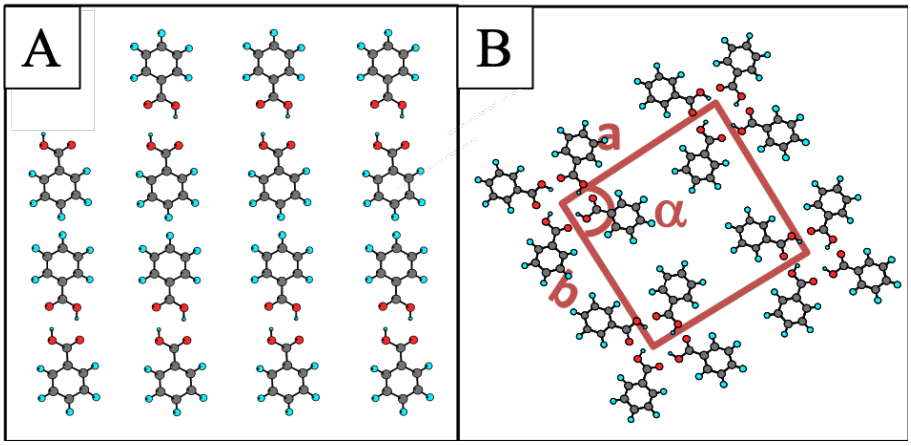

Figure 5.10: (A) is a PowerPoint cartoon of how the linear stripe pattern might be forming due to the H-bonding dimerization of BZA. (B) is a PowerPoint cartoon of how the zigzag pattern might be forming due to the H-bonding tetramerization of BZA. Where both A and B are at the flat orientation of BZA.

Lastly, in region IV, it was hypothesized that similar to TMA, that at the region in the most positive potential window, there would be an upright orientation of BZA. Like, TMA, there is a deprotonation of one CAFG (in the case of BZA it is deprotonation of the only CAFG) which this carboxylate group binds to the substrate. In the case of TMA, this type of binding caused an order SN pattern of a high surface coverage of oval shapes, that form linear features. Similarly, this too was observed with BZA, the comparison of the two features can be seen in Figure 5.11.

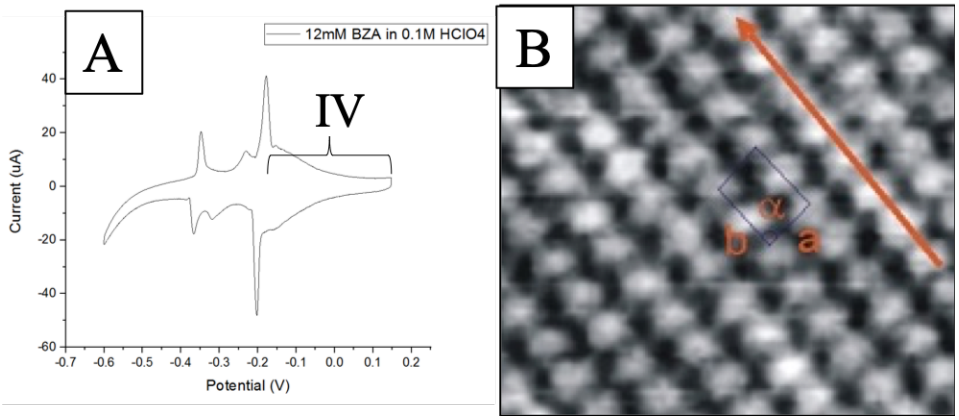

Figure 5.11: (A) CV measured of 12 mM BZA in 0.1 M $HClO_4$ from 0.150 V to -0.200 V, (B) is a 10 nm x 10 nm EC-STM image at E_S = 0.400 V found in region IV where a linear pattern is indicated by the red

arrow. This image has a higher surface coverage of BZA in comparison to Figures 5.7, 5.8, and 5.9. Additionally, the morphology of the BZA molecules suggest that like in the literature the BZA molecules are upright, covalently bonded to the substrate after deprotonation of the CAFG.

5.4: CHAPTER FIVE REFERENCES

1. Horcas, I.; Fernandez, R.; Gomez-Rodriguez, J. M.; Colchero, J.; Gomez-Herrero, J.; Baro, A. M., WSXM: a software for scanning probe microscopy and a tool for nanotechnology. *Rev. Sci. Instrum.* **2007,** *78* (1).
2. Hegner, M.; Wagner, P.; Semenza, G., Ultralarge atomically flat template-stripped Au surfaces for scanning probe microscopy. *Surface Science* **1993,** *291*, 39-46.
3. De Feyter, S.; De Schryver, F. C., Two-dimensional supramolecular self-assembly probed by scanning tunneling microscopy. *Chem. Soc. Rev.* **2003,** *32* (3), 139-150.
4. Nicholson, K. T.; Minton, T. K.; Sibener, S. J., Temperature-dependent morphological evolution of HOPG graphite upon exposure to hyperthermal O(^{3}P) atoms. *Progress in Organic Coatings* **2003,** *47* (3-4), 443-447.
5. Teschke, O., Imaging Ice-Like Structures Formed on HOPG at Room Temperature. *Langmuir* **2010,** *26* (22), 16986-16990.
6. Li, Z.; Wan, L. J.; Wandlowski, T., Supramolecular Nanostructures of 1,3,5-Benzene-tricarboxylic Acid at Electrified Au(111)/0.05M H_2SO_4 Interfaces: An in Situ Scanning Tunneling Microscopy Study. *Langmuir* **2005,** *21* (15), 6915-6928.
7. Jadzinksy, P. D.; Calero, G.; Ackerson, C. J.; Bushnell, D. A.; Kornberg, R. D., Structure of a Thiol Monolayer-Protected Gold Nanoparticle at 1.1 Å Resolution. *SCIENCE* **2007,** *318*.
8. Lehmann, M. S.; Feld, R.; Muir, K. W.; Speakman, J. C., The crystal structure of Benzoic Acid: a redertimination with X-rays at room temperature; a summary of neutron-diffraction work at temperatures sown to 5K. *Zeitschrift für Kristallographie* **1981,** *157*, 215-231.
9. Bruno, G., A Refinement of the Benzoic Acid Structure at Room Temperature. *Acta. Cryst.* **1980,** *B36*, 1711-1712.
10. Wilson, C. C.; Shankland, N.; Florence, A. J., A single-crystal neutron diffraction study of the temperature dependence of hydrogen-atom disorder in benzoic acid dimers. *J. Chem. Soc., Faraday Trans.* **1996,** *92* (24), 5051-5057.

CHAPTER 6: SUMMARY

6.1: CONCLUSION

This fundamental study focuses on the molecular building blocks of BZA, a AH, and its solid/liquid interface interaction with a Au substrate. More formally, this electrode/electrolyte interface study attempted to study the two dimensional supramolecular self-assembly of the BZA building blocks. Studying the effects of the self-assembly of BZA on a Au(111) substrate at the electrode/electrolyte interface with EC-STM and CV is the unique and a significant novelty behind this work. Though, similar works have been done[1-3], for example, TMA on a Au(111) substrate with EC-STM.[4-6]

These two compounds, BZA and TMA, are very similar, they are both AH with CAFGs. Where BZA has only one CAFG and TMA has three where the fewer CAFG has shown to add to the difficultly of making observations of ordered adsorption phases which most likely due to it only having one CAFG. The formation of the SNs are largely dictated by the H-bonding intermolecular interactions that take place in both studies. BZA, however, has less opportunity to make as many H-bonding interactions due to the same fact that BZA has less CAFGs.

Yet, with this difficulty and the previous work with TMA, it was still hypothesized that certain observations would be made. These hypotheses were a flat and an upright orientation of the adsorbed BZA adlayer based on different induced potentials. What wasn't hypothesized was the lack of ordered adsorption phases when using a similar molecular concentration (3 mM) in a similar electrolyte solution (0.05 M H_2SO_4) and on a similar substrate. Similarly, the lack of adsorption/desorption peaks in the CV measured at this concentration.

Originally, it was thought that perhaps there is an electrolyte effect competing with the BZA in the adsorption and as a result the electrolyte solution was switched to $HClO_4$. Still a similar

observation was made with disorder adsorption phases observed. At this point, it was thought that perhaps the concentration of BZA needed to be increased. It was increased to 20 mM BZA in 0.1 M $HClO_4$ and this led to the observation of multiple peaks in the CV which allowed for more potential regions to observe different adsorption phases.

However, there was still the problem of not knowing when the concentration was to little versus when is the concentration enough to make the same observations. This led to the study the CV experiments of varying the concentration of BZA in 0.1 M $HClO_4$, where the transition concentration was found at 6 mM BZA. As the concentration increased it was found that the peaks became more distinguished and increased in separation. This CV study was not done for the H_2SO_4 due to a lack of time, however, perhaps there is a transition concentration for this electrolyte as well. If it is at the same concentration (6 mM) for this electrolyte, then perhaps the electrolyte does not affect the formation of the SNs, perhaps it is affected more by the lack of CAFGs that allow for more H-bonding. Alternatively, maybe the opposite is true, the experiment needs to be done to validate or deny these possibilities.

It was found that similar to TMA, there are flat and upright orientation of BZA observed at negative and positive induced potentials, respectively. However, the flat orientation structures allow for the comparison to the crystal structure of BZA and at regions II and III in the CV of 12 mM BZA in 0.1 M $HClO_4$. Where region IV, the upright orientation, is incredibly similar to that of TMA. Lastly, region I was found to be a disordered phase much like the previous observations with the lower concentrations of BZA in either the $HClO_4$ or the H_2SO_4 electrolyte.

Fortunately, the goals within the project appear to be met with BZA and it can be speculated that the individual that will continue this project might move on to another compound of interest. It was concluded that the molecule-molecule interaction was largely dictated by the strong

intermolecular interaction of H-bonding between CAFGs of the adjacent BZA molecules. The molecule-substrate interaction seems to be largely dictated by how the AH binds to the Au surface at the flat orientation and the binding of the carboxylate group to the Au surface at the negative potential and the positive potential, respectively. Additionally, there at least three parameters that can now be thought of when trying to observe the self-assembly of organic compounds on a metal substrate, where the concentration of the organic compound and the electrolyte the organic compound is dissolved largely affects the ability to observe multiple SNs. Whereas, the potential applied to the substrate affects how to transition from one adsorption phase to another. However, it should be repeated that the smaller number of functional groups that allow for intermolecular interactions, such as CAFGs, the more difficult it could be to observe ordered SNs and thus the three effects/parameters must be explored.

6.2: CHAPTER SIX REFERENCES

1. Vu, T.-H.; Wandlowski, T., CV and in situ STM study the adsorption behavior of benzoic acid at the electrified Au(100)| HClO4 interface: Structure and dynamics. *Journal of Electroanalytical Chemistry* **2016,** *776*, 40-48.
2. Vu, T.-H.; Wandlowski, T., Self-Assembled Structures of Benzoic Acid on Au(111) Surface. *Journal of Electronic Materials* **2017,** *46* (6), 3463-3471.
3. Kim, Y. G.; Yau, S. L.; Itaya, K., In Situ Scanning Tunneling Microscopy og Highly Ordered Adlayers of Aromatic Molecules on Well-Defined Pt(111) Electrodes in Solution: Benzoic Acid, Terephthalic Acid, and Pyrazine. *Langmuir* **1999,** *15*, 7810-7815.
4. Li, Z.; Wan, L. J.; Wandlowski, T., Supramolecular Nanostructures of 1,3,5-Benzene-tricarboxylic Acid at Electrified Au(111)/0.05M H_2SO_4 Interfaces: An in Situ Scanning Tunneling Microscopy Study. *Langmuir* **2005,** *21* (15), 6915-6928.
5. Li, Z.; Wandlowski, T., Structure Formation and Annealing of Isophthalic Acid at the Electrcochemical Au(111)-Electrolyte Interface. *J Phys Chem C* **2009,** *113*, 5.
6. Clair, S.; Pons, S.; Seitsonen, A. P.; Brune, H.; Kern, K.; Barth, J. V., STM study of terephthalic acid self-assembly on Au(111): Hydrogen-bonded sheets on an inhomogeneous substrate. *J. Phys. Chem. B* **2004,** *108*, 14585-14590.

APPENDIX

APPENDIX A: ATOMIC FORCE MICROSCOPY

APPENDIX A.1: AFM EQUIPMENT AND WORKING PRINCIPLE

AFM is quite different from STM, however, if it was boiled down to one major difference it would be that there is no need for the sample or substrate to be conductive. There are multiple differences between STM and AFM, however, this has to be the most fundamental difference. This is because the imaging technique does not rely on quantum tunneling in order to develop an image. Instead, it uses a laser and constantly measuring how the laser is moves as it is reflected onto a photodiode to develop an image. Before going into some further detail on the inner workers of this instrument, it needs to be expressed further differences between the two SPM techniques. This will be done by listing the major equipment necessary to perform an AFM measurement and then how these parts work as a whole to development an image.

The first piece of equipment that should be addressed is the AFM probe, where this probe is not manufactured by this group. Instead, the probes are purchased from NanoWorld as a pack of 50 at a time. This probe is a relatively small silica chip that holds a flexible cantilever which hangs over the edge of the silica chip. The probe is on the cantilever, however, cannot be seen by the naked eye due to how small it is, refer to Figure A.1 for a visual representation of the AFM probe as a whole.

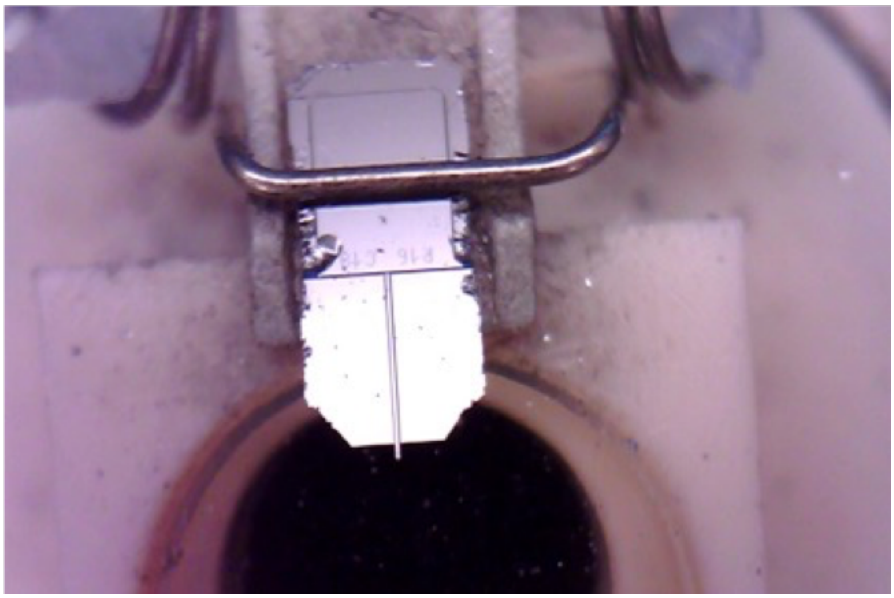

Figure A.1: NanoWorld AFM Probe mounted onto the AFM scanner nose.

This AFM probe is mounted onto the next piece of equipment, the AFM scanner. This scanner, like the STM scanner, has a PEM built into it. This PEM is used in a similar circuit loop like that with STM for measuring the current produced from quantum tunneling, however, like it was stated earlier AFM does not rely on quantum tunneling, therefore, it does not measure the current produced from this phenomenon. Instead, it measures the force exerted onto the AFM probe when the probe is close enough to the sample to be repulsive or far enough away from the sample yet still close to the sample to be attractive, with respect to the anhormonic oscillator model. Dissimilarly the STM scanner, the AFM scanner has a laser built into the scanner with optical lenses to help focus the laser to a fine point such that it can be shined on the back of the cantilever, behind the probe. The light from the laser is then reflected back to a slot in the AFM scanner that hold the photodiode.

The photodiode is a small attachment that connects to the scanner after the laser has been pre-aligned properly. Where a feature of the photodiode has a grid much like that of a graphing grid where there are four quadrants I, II, III, and IV. Where quadrant I is the positive x- and y-axis,

quadrant II is the negative x-axis and the positive y-axis, quadrant III is the negative x- and y-axis, and quadrant IV is the positive x-axis and the negative y-axis. Where the laser is aligned in such a way to maximize the reflective signal and to be at the center (origin) of the photodiode grid.

All the AFM equipment listed at this point are all integrated to one another and also into the instrument in replace of the STM scanner, that is the apparatus that sits in the Faraday box can be used for both SPM techniques previously discussed. The next set of equipment will be the last major piece needed for measurements. There are other pieces of equipment other than what is about to be discussed but is not absolutely necessary for developing imaging measurements. This type of equipment can be thought of as convenience pieces and are not necessary when using the NanoWorld AFM probes. This equipment includes but are not limited to the AFM camera (sits above the AFM scanner in the Faraday box, pointed at the AFM scanner) and the microscope camera (same one that is used for watching the EC-etching and coating processes for developing STM probes found in Figure 3.11 in Chapter 3).

This next piece of equipment that is necessary to develop an AFM image is the AFM plate. This is very similar to the EC-STM cell plate, except there are not attachments that allow for the circuit to be connect to the apparatus in the Faraday box, nor is there a circuit on the plate itself. In fact, the AFM plate has two holes for the guiding rods (used to allow for only one type of movement of the cell plate, the z-direction), two large metal clamps to hold the substrate in place, and a hole in the middle of the plate such that an attachment may be added to the AFM plate.

APPENDIX A.2: SUBSTRATES/SAMPLES AND THEIR PREPARATIONS

The requirements of a substrate for the AFM technique is something that is relatively flat and can be easily cleaned. Where the contamination issue that is experienced throughout EC-STM or EC-CV is not as prevalent. Where one substrate that has been used for the projects that AFM is

used for is known as Mica, which is also known as Muscovite.[1-2] Cleaning this substrate is quite easy, where one only needs the substrate itself and Scotch tape to cleave layers of contaminates that may have settled onto the substrate and layers of the substrate itself.[3] Where the goal is to cleave one solid layer so that it appears relatively flat to the naked eye. Where if the experiment calls for imaging Mica only, then the AFM plate can be integrated for making measurements, or, if the experiment calls for imaging nanoparticles deposited onto the substrate (for example) then one can do that and allow the solution to dry before integrating into the instrument to make the measurements. Lastly, it should be noted the type of AFM technique that is used for the AFM projects, what those projects are, and who was performing the experiments.

There are two major types of AFM techniques, they are contact and non-contact scanning modes, where the non-contacting mode. Where contact mode has the probe touching the substrate and is dragged across the surface of the substrate so that an image can be developed, which is potentially more damaging to the substrate and the sample. Non-contact mode is relatively safer for the substrate to use because it doesn't interact with the surface to the same extent as the contact mode does. The non-contact mode makes the cantilever oscillate with a certain frequency, gently tapping at the surface as it scans over the substrate, which is used to develop an image. The non-contact mode has to go through an Acoustic (AC) Auto-tune measurement before imaging to test the AFM probe's ability to image. That is, to make sure the AFM probe is not damaged. Throughout the AFM projects, the non-contact or tapping mode used to develop the AFM images.

The individuals that were performing the experiments were Cody Leasor, who trained and performed the experiments in each project with four undergraduates using this SPM technique, they are Kelsi Goshinksy, Malachi Jones, William Borely, and Sara Biallas. Where none of the samples that were measured with these individuals, were prepared by these individuals. The

samples vary depending on the project, where there are three projects: Imaging CISD2 protein which was prepared by Dr. Konkle's group, Solar cell electrodes prepared by Maggie Sutten from Dr. Li's group, and $NiWO_4$ nanoparticles (NPs) developed by Andrew Riley from Dr. Li's group. Where the goal was to familiarize everyone with the various samples that can be imaged by AFM and the techniques to perform the imaging measurements that are required of each sample, as a collaboration to provide data of the various samples.

APPENDIX A.3: IMAGING CISD2 PROTEIN

Imaging the CISD2 protein came with a well-defined restriction, that was there was a very limited amount that can be used for imaging. This solution was separated into small centrifuge containers for the convenience of not needing to melt the entire stock solution at a time for each experiment or trial of imaging this sample. Where it was thought that Mica might be a good substrate to use as it was not foreseen to produce any issues. The nature of research though, often comes with unforeseen issues, one such issue is that Mica has a charge at certain pH values that might be hindering the observations of the protein's morphology.[4] The solution was prepared by Dr. Konkle's group by the procedure found within previously published work that involve the expression and purification of mitoNEET, which was produced to have a pH of 7.[5] Where the protein is known to have a large positive charge regions and large negative charge regions which can be seen in the work with NEET proteins from Tamir, S. et al.[6]

The charge of the Mica based on the protein solution pH value was hypothesized it had such an interaction that the shape of the protein was not observed well, as it was quite difficult to distinguish it from possible contaminants, refer to Figure A.2 for a couple examples AFM images of the protein.

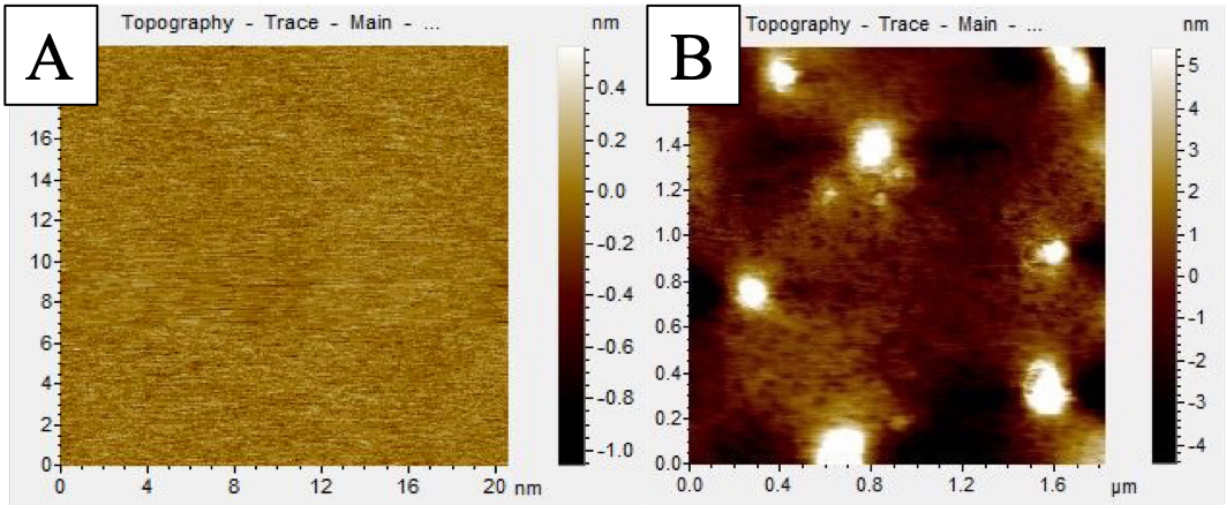

Figure A.2: (A) 20 nm x 20 nm of Mica from using the NanoWorld probe in ACAFM mode that shows that the surface is relatively flat. (B) indistinguishable features in the 1.8 µm x 1.8 µm AFM image of the CISD2 protein deposited on Mica and images in ACAFM mode.

Additionally, there were not any observations of very dense amount of protein in a given area of the images developed. The combination of these possible issues led the group to switch directions of this project to use a different substrate that won't change its charge based on pH. This new substrate is a SAM of thiolated organic compounds on Au(111) (the same crystal used in EC-STM projects previously stated). However, there has not been enough time to further investigate this method of imaging the protein. Thus, this is a plan for future experiments with AFM.

APPENDIX A.4: IMAGING Au and $NiWO_4$ NANOPARTICLES SEPERATELY

Imaging $NiWO_4$ NPs that Andrew had developed was used with another Microscopy technique, which was TEM. Where both techniques have their strengths, yet, AFM offers more information to be measured because of its ability to make a three-dimensional image of the surface rather than TEM which projects a two-dimensional image of the NPs' shadow. The $NiWO_4$ NPs that were imaged with AFM were prepared by Andrew where 0.04 M Na_2WO_4 was mixed with 0.85 grams of Sodium Dodecyl Sulfate (SDS) and 25mL of water. Then the $NiWO_4$ NPs

precipitated out after adding a solution of 0.05 M $AgNO_3$ and 0.1 M $Ni(NO_3)_2$ solution mixed with 0.035 grams of SDS. After washing with ethanol and water the NPs were calcinated in air at 230°C.

After the $NiWO_4$ NPs were prepared by Andrew, 4.3 milligrams of the NPs were then placed in a vial that contained roughly 40 drops of chloroform and mixed thoroughly to get as much of the NPs suspended into solution as possible. This solution was used to deposit as much of the NPs as possible onto the cleaned Mica substrate where the chloroform evaporated quickly and all that remained were the NPs and/or possible contamination on the substrate. This was the general procedure for introducing the NPs (listed above) onto the surface of Mica. The resulting images can be found in Figure A.3.

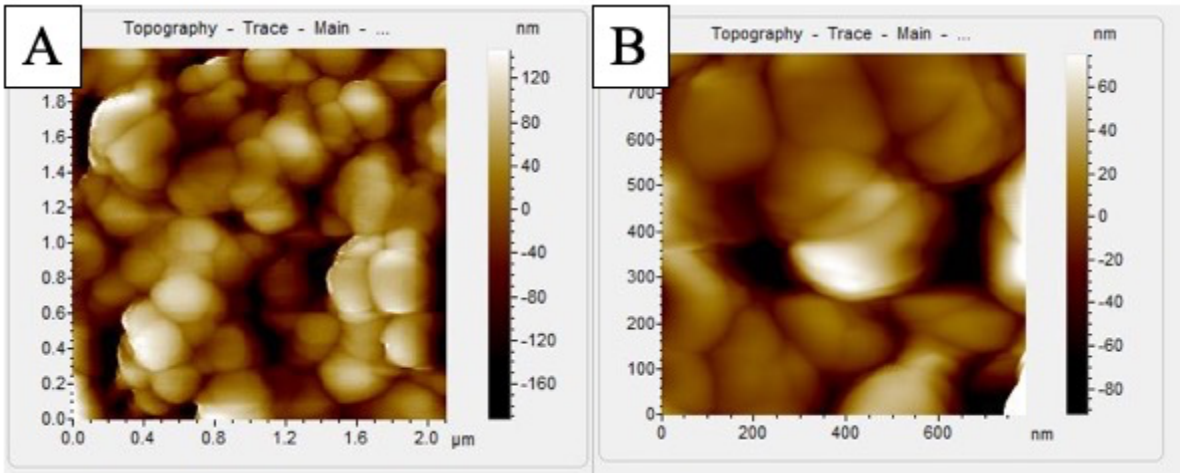

Figure A.3: (A) 2.0 µm x 2.0 µm ACAFM mode image of $NiWO_4$ NPs deposited on freshly cleaved and cleaned Mica. (B) 800 nm x 800 nm ACAFM mode image of $NiWO_4$ NPs.

There is a method of testing the NPs to see if they are hollow by crashing the tip into a NP and imaging the result of that crash. Unfortunately, again, there was a lack of time to further explore this and as a result will be attributed to a possible future experiment. The Au NPs, however, were also developed by Andrew; where the preparation for these NPs was done by using the Brust-

Schiffrin method.[7] The solution of the NPs was deposited on freshly cleaved/cleaned Mica and let dry before the AFM images were collected, which can be seen in Figure A.4.

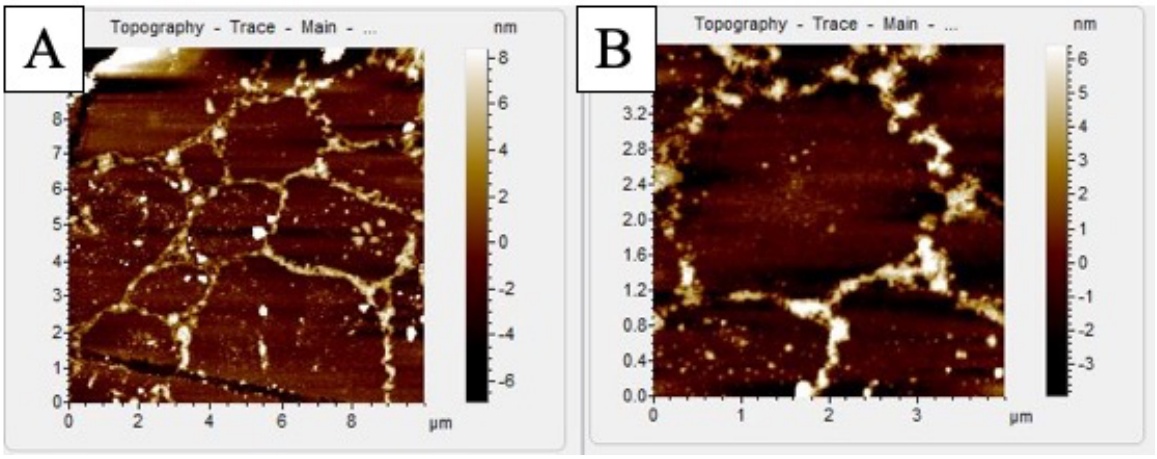

Figure A.4: (A) 10 µm x 10 µm ACAFM mode image of Au NPs deposited on freshly cleaved and cleaned Mica. (B) 4 µm x 4 µm ACAFM mode image Au NPs.

APPENDIX A.5: NANOSENSORS' AFM PROBES VS. NANOWORLD'S AFM PROBES

All of the images that are previously discussed with respect to AFM were collected with the use of NanoWorld brand tips. However, it was been good fortune that this group was given 10 AFM probe samples from the Nanosensors company. The probes from Nanosensors are supposedly better than NanoWorld due the fact that each chip on the Nanosensors' probe has three cantilevers with three probes, one for each cantilever. This results in the Nanosensors' probes are equivalent to three NanoWorld's probes because the NanoWorld's probe contains only one respective cantilever and probe, see Figure A.5.

Figure A.5: Nanosensors' AFM Probe where it can be seen on the right side of the image that there are a total of three cantilevers that hold three imaging probes.

Unfortunately, no discernable image was made with the Nanosensors' probes and is under further investigation and due to time, there hasn't been a resolution to this problem and will be addressed in the near future.

APPENDIX B: DEVELOPMENT OF STM PROBES

There was quite a large number of probes that were made by the EC-etching process, however, not all could have been used as they did not seem sharp enough to move on to the next step when evaluated underneath an optical microscope. In fact, there were a total of 84 probes that were etched throughout two years. Where only 54% made it to the coating step. This left 45 of tips that were used to try and coat so that they can be used throughout EC-STM experiments. Where only 62% of those EC-etched tips were coated well enough for experimentation, which means roughly 28 might have been used for experimentation.

This, in one's opinion, speaks volumes to the difficulty of developing super sharp STM probes and being able to coat them such that they can be used for experimentation. Where, of the total 84 of potential probes only 33% were good enough throughout the two years for this project. It should be noted that this number would be much worse, and the quality of the tips would most

likely be lower without the help and use of the new EC-etching and coating apparatus. See Chapter 3 for how the apparatus implicated the coating in a positive manner when comparing the old apparatus to the new one.

APPENDIX C: DEVELOPMENT OF ARGON TANK APPARATUS

In order to dry some of the cleaned EC-STM equipment a heat gun was used for the development of the Argon Tank apparatus. This could have been a good source of contamination due to fast movement of air allow dust to be picked up and scattered throughout the room from the air flow. Improving this potential problem was a goal for this lab and with the help from Jon Hatton, an Ar tank was set up in the lab with tubbing designed to allow for a split stream of Ar gas to flow. Where one stream could be closed off when one stream was preferred over the other. Stream one, is where the end of hose is connected to a glass pipette for the fine drying of small equipment. Whereas, stream two is connected to a glass funnel for the purpose of cooling Au, however, this has not been developed enough for this stream's intended use. This has shown to produce relatively clean results with STM and thus seems more reliable than a heat gun.

APPENDIX D: IMPROVING Au ANNEALING PROCESS

Improving the drying procedure was not the only goal of this lab, where the Au annealing process can also be improved upon. Where the current procedure is to hold the Au crystal with tweezers and shaking the crystal in a butane flame, then once annealed to the correct temperature for roughly three minutes it is then quenched with Milli-Q water. This is very problematic as it is a risk that at any point the crystal could drop and become damaged if not held properly with the tweezers for an extended amount of time.

Thus, there are two methods in development to improve this procedure. Where method one is to purchase a high heat resistive plate so that the Au crystal can sit on this plate and be flame

annealed. Afterwards, steam of the Ar tank apparatus (see Appendix C) could be cooled for the formation of Au(111). The other method would use a unique piece of glassware to allow H_2 gas to bubble out of Milli-Q water so that a gentle hydrogen flame could be used for the flame annealing of the Au crystal. Once annealing of Au crystal is done then it can be immediately quenched in the H_2 bubbling water. See Figure A.6 These are currently under development and are in the hopes of testing in the near future.

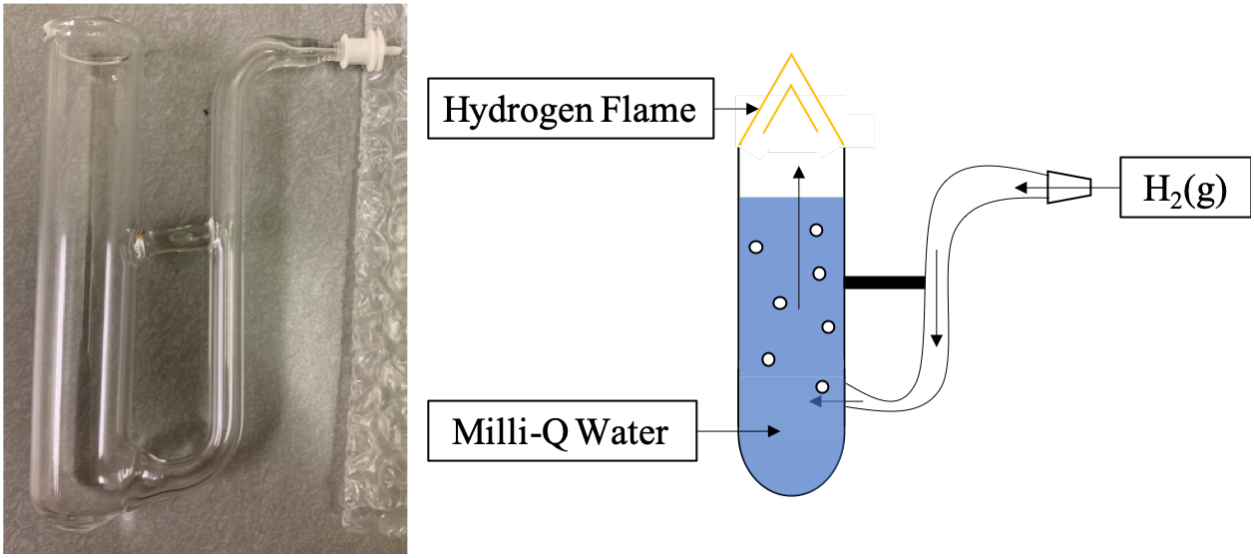

Figure A.6: (A) is an image of the glassware that will be used in combination of the H_2 tank apparatus where (B) is a PowerPoint cartoon of how the flame will be produces for flame annealing the Au crystal. Lastly, because the Au crystal has a tail, immediate quenching can take place submerging the crystal into the Milli-Q water and hooking it to the side of the glass with the tail.

APPENDIX E: TABLE OF FIGURES

APPENDIX F: REFERENCES

1. Miller, C. F.; Stoddard, E. F.; Bradfish, L. J.; A.D., W., Composition of Plutonic Muscovite: Genetic Implications. *Canadian Mineralogist* **1981,** *19*, 25-34.
2. Guggenheim, S.; Chang, Y.; Groos, A. F., Muscovite dehydroxylation: High-temperature studies. *American Mineralogist* **1987,** *72*, 537-550.
3. Ostendorf, F.; Schmitz, C.; Hirth, S.; Kuhnle, A.; Kolodziej, J. J.; Reichling, M., How flat is an air-cleaved mica surface? *Nanotechnology* **2008,** *19* (30).
4. Lee, S. S.; Fenter, P.; Park, C.; Sturchio, N. C.; Nagy, K. L., Hydrated Cation Speciation at the Muscovite (001)-Water Interface. *Langmuir* **2010,** *26* (22), 16647-16651.
5. Roberts, M. E.; Crail, J. P.; Laffoon, M. M.; Fernandez, W. G.; Menze, M. A.; Konkle, M. E., Identification of Disulfide Bond Formation between MitoNEET and Glutamate Dehydrogenase 1. *Biochemistry* **2013,** *52* (50), 8969-8971.
6. Tamir, S.; Paddock, M. L.; Darash-Yahana-Baram, M.; Holt, S. H.; Sohn, Y. S.; Agranat, L.; Michaeli, D.; Stofleth, J. T.; Lipper, C. H.; Morcos, F.; Cabantchik, I. Z.; Onuchic, J. N.; Jennings, P. A.; Mittler, R.; Nechushtai, R., Structure-function analysis of NEET proteins uncovers their role as key regulators of iron and ROS homeostasis in health and disease. *Biochim. Biophys. Acta.* **2015,** *1853* (6).
7. Liz-Marzan, L. M., Gold nanoparticle research before and after the Brust-Schiffrin method. *Chem. Commun.* **2013,** *49* (1), 16-18.